ANNALS OF GEOPHYSICS, 66, 5, DM532, 2023; doi:10.4401/ag-8981
OPEN ACCESS

Sediment-thickness and upper-lower crustal boundary of the Maracaibo block, Venezuela, from gravity study

Francisco Araujo[*,1,2], Nuris Orihuela[1]

(1) Universidad Central de Venezuela Departamento de Geofísica

(2) Petróleos de Venezuela, Instituto de Tecnología Venezolana para el Petróleo (PDVSA Intevep) Gerencia de Exploración y Caracterización de Yacimientos

Article history: received May 16, 2023; accepted December 7, 2023

Abstract

The Maracaibo Block is a triangularly shaped fraction of independent continental lithosphere located in north-western Venezuela, controlled by a complex system of strike-slip and thrusts faults; the Oca-Ancon fault (north), the Santa Marta-Bucaramanga fault (southwest) and Boconó fault (east). In the present research we study two interfaces associated with the upper crust, the basement-sediment, and the upper-lower crustal interface, as well the interaction with the Caribbean plate. These interfaces were defined using gravimetric inversion methods in conjunction with well information, refraction and reflection seismic and seismological data. Applying the inversion algorithm of Cordell and Henderson to the gravimetric data, 10 km of sedimentary column are estimated in the deepest part of the Maracaibo Lake basin and 5 km in the Apure Barinas basin, both zones coincide with the minimum gravimetric anomaly of each basin. Using spectral analysis, a discontinuity with depths between 17 and 24 km is observed; located between the upper and lower crustal boundary. Four gravimetric domains are defined; to the north related to the displacement of the Oca-Ancon fault and its influence on the Bonaire block, to the west the displacement of the Santa Marta Bucaramanga fault, to the east the Apure fault and the central domain, relacionated with the Maracaibo block. There are 60 km of distance between the gravity minimums belonging to the Apure Barinas and Maracaibo Lake basins; this displacement is associated with the right lateral strike slip offsets of the Boconó fault. The displacement of Boconó fault, and the shortening in a northeast-southeast direction, is consistent with ongoing strain partitioning in the Mérida Andes. A displacement of 110 km is proposed for the Santa Marta Bucaramanga fault and 100 km for the Oca Ancon fault, respectively. The first pulses of Oligocene uplift of the Merida Andes are due to the interaction of the Maracaibo block with the Caribbean plate. The uplift of the Merida Andes was dominated mainly by the northwest-southeast compression until 4 Ma ago; in the Pleistocene, the displacement of the Boconó fault and the rotation of the Trujillo block began to control the current structural configuration of the northeastern Mérida Andes. This interaction gives rise to a pattern of gravimetric lows and highs associated with subbasins and basement highs, located between Oca Ancón and Boconó faults.

Keywords: Maracaibo Block, Gravity, Boconó Fault, Apure Barinas Basin, San Lazaro Graben

1. Introduction

The gravimetric study of the geometry of the sedimentary basins along both flanks of the Merida orogen, as well as the influence of the Andean fault system on these, will allow a better understanding of the geology of the Maracaibo Block. Due to the complex interaction of plate motion involving several plates with pre-existing structures, as well as the absence of deep crustal seismic data, their structure and kinematics remain controversial. In 2013, the Integrated Geoscience of the Mérida Andes Project (GIAME) was carried out with the intention of improving the geological image at the lithospheric scale, through the use of seismic refraction, reflection, seismology and gravity data. The main objective of this research is to investigate the relative movement of the main fault systems that border the Maracaibo block and that have influenced the growth of the mountain systems and the geometry of the Apure Barinas and Lake Maracaibo basin. The first step consisted in the compilation of the complete Bouguer anomaly (CBA) map, through the merger of surveys acquired in 2005, 2006 [Tupure Carora Project; Moncada et al.,2006], 2013 and 2014 for Integrated Geosciences of the Mérida Andes Project [GIAME; Schmitz et al., 2015], by institutions as Petroleos de Venezuela (PDVSA Intevep), Fundación Venezolana de Investigaciones sismologicas (Funvisis), Universidad Central de Venezuela (UCV). After we proceeded to join these acquisitions with existing surveys since the 1970s, for which a homologation of all data had to be carried out [Araujo and Orihuela 2020]. Using spectral analysis of the gravimetric anomaly, the depth of the upper crust-lower crust interface is obtained, and from the application of the Cordell and Henderson [1973] algorithm to the residual CBA, together with well information, the basement sediment interface was defined. The depth of the metamorphic igneous basement is of great interest in oil exploration, since it shows the thickness of the sedimentary column. While the upper and lower crust interface is important from the seismological point view. Since most seismic events due to the movement of fault planes occur in this layer. However, the gravimetric method presents many degrees of freedom, when we do mathematical inversions, for this reason the gravimetric data is integrated with well information, seismic reflection and seismological information, to reduce the number of solutions and thus obtain a better model of subsurface.

The Maracaibo Block (MCB) is a fraction of independent continental lithosphere triangularly shaped located in north-western Venezuela, belonging to the North Andes plate [Pérez et al., 1997, 2018; Figure 1]. This plate together with the Maracaibo block is currently being extruded to NNW with respect to South America [Bird, 2003; Trenkamp et al., 1996] (Figure 1). The MCB block is bounded by the left-lateral Santa Marta-Bucaramanga fault system to the west; the right-lateral Boconó fault system, to the east, and limited on the north by the right lateral strike slip Oca-Ancon fault system, Bonaire block (BB) and the south-Caribbean deformed belt, to the north [Mann and Burke, 1984]. This region has been interpreted as an escaping continental block squeezed in an area of intra-continental shortening [Backé et al., 2006] as a consequence of the late-Neogene west to east collision of the Panamá arc with north-western South America [Mann et al., 1990; Audemard and Audemard, 2002]. The Maracaibo Block is cut by a series of N-S left-lateral strike-slip faults separating several crustal units [Audemard et al., 2000; Escalona and Mann, 2003; Mann et al., 2006]. Among these, the most important is the eastern most Trujillo Block (TB) [Hervouët et al., 2001]. Bounding this continental block are the Sierra Nevada de Santa Marta, Perijá, Mérida Andes (MA), and Macizo de Santander mountain belts includes the Maracaibo and Rancheria basin. These belts were formed by complex geodynamic interactions between the Caribbean Plate, the Panamá Arc, and the South American Plate, which resulted in the reactivation of major preexisting structures or inherited discontinuities. The Merida Andes (or Venezuela) formed by complex geodynamic interaction between the Caribbean Plate, the Panamá Arc, the South American Plate and the continental Maracaibo block. This orogeny result from rotation and oblique convergence between the Maracaibo continental block to the north and the South American plate to the south [Case et al., 1990; Colletta et al., 1997; Montes et al., 2005; Pindell and Kennan, 2009]. Convergence started in the late Paleogene and resulted in major surface uplift, evolution of the drainage pattern and exhumation of the Venezuelan Andes during the late Miocene [Kohn et al., 1984; Hoorn et al., 1995; Bermudez et al., 2010, 2011, 2013]. The growth of the Venezuelan Andes apparently caused the separation of the Maracaibo and Apure Barinas basins [Guzman and Fisher, 2006], which previously formed a continuous basin bounded by the northern Andes in Colombia to the northwest and west and the Guyana Shield to the southeast (Figure 1).

The Miocene-Pliocene flexural subsidence was caused by crustal loading of the rising Merida Andes [De Toni and Kellogg, 1993]. This move in regional plate kinematics may have been driven by collision of the Panama arc with the northern Andes in Colombia [Kohn et al., 1984; Colletta et al., 1997], resulting in clockwise rotation of the Maracaibo block and the Santa Marta massif [Montes et al., 2005].

The structure of the Merida Andes, the Sierra Nevada de Santa Marta, Sierra de Perijá, and Macizo de Santander is controlled by a complex system of strike slip and thrusts faults, one of the most important is the Bocono fault; Santa Marta Bucaramanga fault and Oca-Ancon fault.

2. Tectonic setting

The MCB can be considered as the northwestern most fragment of the Guiana Shield, overlain by extensive Phanerozoic supracrustal sequences. During the late Cretaceous, the MCB began to migrate northwestward along the Santa Marta-Bucaramanga and Oca fault systems [Figure 1; Pindell, 1993]. Transpressional forces generated during this process resulted in the development of different tectonic blocks such as the Mérida Andes, the Caparo block, and the Serranía de Trujillo or Trujillo block within the Venezuela Andes.

The oblique convergence between the Maracaibo Block and the Guyana shield has led to strain partitioning along the Mérida Andes [e.g. Rod, 1956; Colletta et al., 1997; Audemard and Audemard, 2002; Audemard, 2003; Audemard et al., 2006], divided between (1) shortening perpendicular to the belt and which causes uplift and development of the Northern and Southern Thrust Systems fault, (2) right-lateral strike-slip movement along the Boconó Fault, and (3) the partition and tectonic escape of the Trujillo Block [Backé et al., 2006]. The NNE extrusion of the Maracaibo Block with respect to South America caused this block to override the Caribbean plate north of the Leeward Antilles Islands, where a young south-dipping, amagmatic, flat oceanic subduction of low dip in south direction has been forming in the last 5 Ma [Audemard et al., 2000].

2.1 Santa Marta Bucaramanga Fault System

The NNW striking left lateral strike-slip Santa Marta-Bucaramanga Fault System (SMBF) is the most prominent fault system in the northern part of the Colombian Andes, north of 6.5°N latitude. Presently forms the active western boundary of the Maracaibo block (Figure 1). Structural restoration along the southern termination of the fault reveals left-lateral displacement on the order of 40 km [Toro, 1990], although total displacement of more than 100 km previously has been proposed [Campbell, 1968; Etayo and Rodrıguez, 1985].

Movement along the Bucaramanga fault resulted in oblique normal uplift to the immediate east in the Santander massif. This uplift continued farther east but was transformed into predominantly thrust-induced thickening in the Serranıa de Perija, a process that began in the Miocene.

2.2 Oca-Ancón Fault System

Since the middle Cretaceous, it has formed the northern boundary fault of the Maracaibo block, and has exhibited right-lateral movement [Feo-Codecido 1972; Vasquez and Dickey 1972; Tschanz et al., 1974; Macellari 1995; Giraldo 1996]. Reconstructions of Maresch et al. [2000] suggest transform capture of the Romeral-San Jacinto systems during emplacement of the Caribbean platein the Paleocene. The Oca-El Pilar system developed a major shear zone, best observed in the Eocene, along which basic and later acidic magmatism was emplaced. The Oca fault alone presents right-lateral displacement estimated at between 65 and 195 km. In the Eocene, the system also acted as a hinge mechanism that permitted the development of a foreland basin along the front of the Maracaibo basin [Lugo and Mann, 1995]. Dextral-oblique obduction of the Caribbean Mountain terrane took place along this structure.

2.3 Boconó Fault System

The NE-SW trending right-lateral-strike-slip Boconó fault runs slightly oblique to the MA chain axis and its north-eastern tip bounds the Caribbean Coast range of northern Venezuela on the west, thus extending for about 500 km between the Táchira depression at the border between Colombia and Venezuela, and Morón on the Caribbean coast of Venezuela [Audemard and Audemard, 2002] At its north end at the coast, the Bocono fault exhibits a 45° clockwise bend that allows prolongation into the east-west striking San Sebastian-El Pilar system (Figure 1). Age

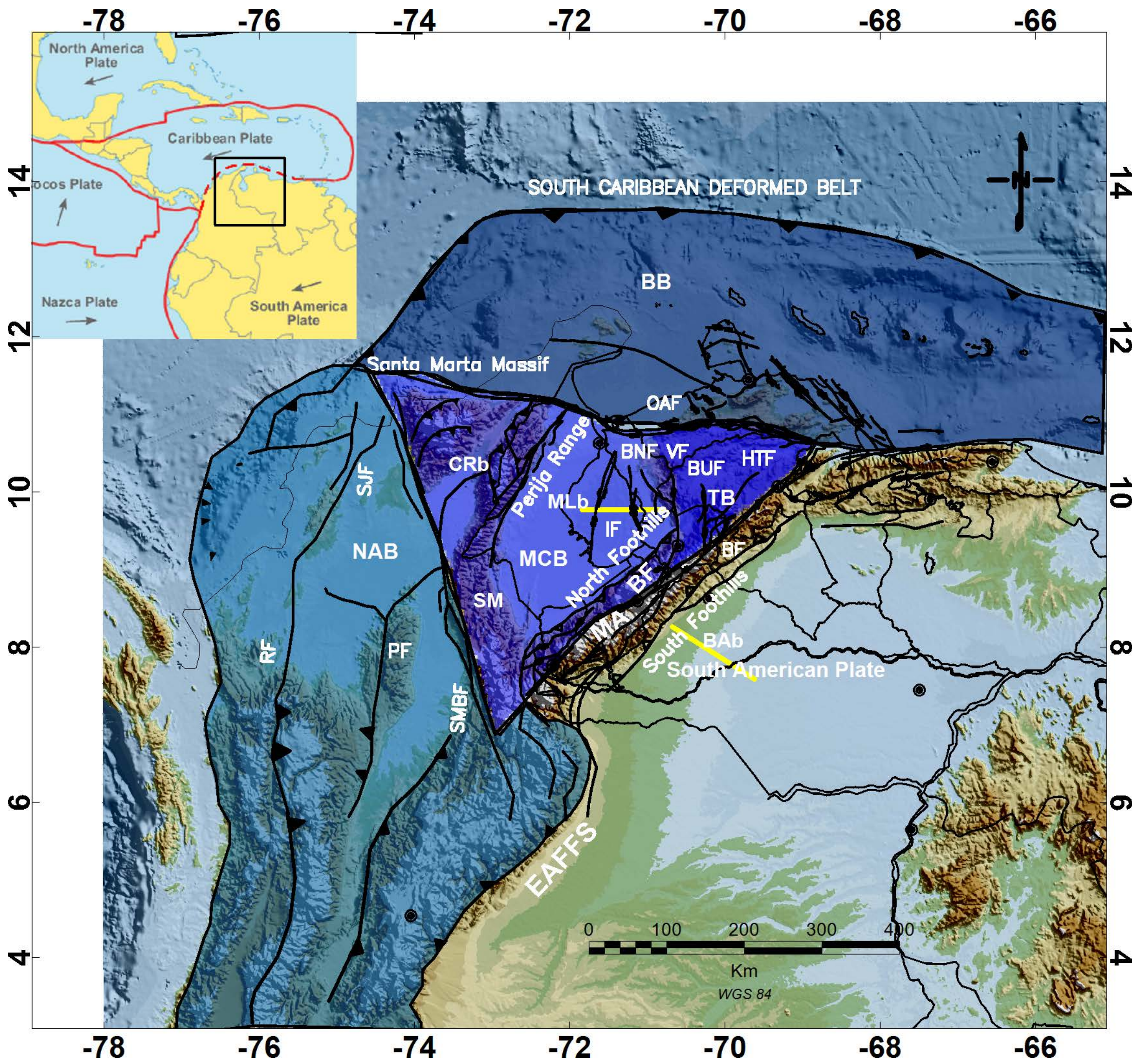

Figure 1. The Maracaibo Block (MCB) with respect to the geodynamic setting of the northern Andes, from Colombia to Venezuela [after Audemard et al., 2000; Audemard and Audemard, 2002; Monod et al., 2010; Escalona and Mann, 2011; Ceron et al., 2007; Cediel et al., 2003; Taboada et al., 2000.] showing the location of the Merida Andes (MA), Perija Range, Santa Marta Massif, Santander Massif (SM). BB = Bonaire Block, TB = Trujillo Block, NAB = North Andean Block, EAFFS = Eastern Andean front fault system, SMBF = Santa Marta Bucaramanga fault, PF = Palestina fault, RF = Romeral fault, SJF = San Jacinto fault, OAF = Oca Ancon fault, BNF = Burro Negro fault, VF = Valera fault, IF = Icotea fault, BUF = Burbusay fault, HTF = Hato Viejo fault, BF = Bocono fault. CRb = Cesar Rancheria basin, MLb = Maracaibo Lake basin, BAb = Apure Barinas basin. Yellow lines represent seismic profile in Maracaibo Lake and Apure Barinas basin. Topographic map is derived from the Shuttle Radar Topography Mission database (SRTM30), and bathymetry from the TOPEX global database [Sandwell and Smith, 1997].

estimates for this structure vary from late Miocene [Audemard and Audemard, 2002], Pliocene [Dewey, 1972], or Pleistocene [Schubert and Vivas, 1993]. Important thrusting also occurs subparallel to the Boconó fault on both sides of the Andes chain, which sustains the mountain's height. Therefore, shear (and slip) partitioning occurs here due to an oblique (east-west) maximum horizontal stress [Audemard et al., 2000]. The estimates of total displacement of the Boconó fault range from 9 km [Schubert, 1993], to 30 km estimated from the offset of the Bouger anomaly [Audemard and Audemard, 2002; Audemard et al., 2007b] and to 80 km estimated from the shift of depositional ages of the Caribbean allochthons [Stephan, 1982].

2.4 Trujillo block

Trujillo triangular block is bounded on the west by the Valera fault and on the south-east by the Boconó fault [Hervouët et al.,2001]. According to Audemard [2003] and Audemard et al. [2000, 2005], the Trujillo block is subjected to a rigid clockwise rotation induced by conjugate movements along the Oca-Ancón and Boconó faults and mimics a bookshelf rotation model. The Trujillo block moves towards the NE as a consequence of conjugate strike slip motions along the Boconó and Valera faults, in a tectonic escape process [Hervouët et al., 2001, 2005; Dhont et al., 2005a].

According to Cruces et al. [2022] a conductive zone was interpreted as the detachment surface in the Trujillo Block. The Trujillo Block, which is bound laterally by the Bocono (BF) and Valera (VF) fault systems, formed as a consequence of the relative convergence between the Maracaibo Triangular Block (MTB) and the Guyana shield. The magnetotelluric results suggest a connection of this conductive detachment zone with the conductive anomalies associated with the Valera fault (VF) and the BF, this detachment is probably located about 16 km deep.

2.5 Bonaire block

The Bonaire block bounded by the Curacao Ridge on the north and the Oca-San Sebastian faults on the south is a small crustal block between the Caribbean, Maracaibo block and South American plate [Silver et al., 1975].

The Caribbean plate is made up mainly of two lithospheric fragments of oceanic crust [Baquero, 2015]. The first fragment is known as the Igneous Province of the Caribbean (CLIP) of late Cretaceous age, with an anomalous thickness between 5-15 km, corresponding to the offshore basins of Venezuela and Colombia; and the second fragment is made up of the Cenozoic basins of Grenada, Bonaire and the Prominence of Aves as part of the Arch of Grenada. In a second fragment it is possible to identify a set of magmatic arc rocks of origin continental. According to Vander Lelij et al. [2010] there was a sequential and diachronous collision of terranes that comprise Aruba, Bonaire and Gran Roque at 70-60 and ~50 Ma resulted in the amalgamation of the Bonaire Block at ~50 Ma. The Bonaire Block has subsequently been entrained within the south Caribbean Plate margin and has been deformed by dextral displacement between the Caribbean and South American plates. Upper Eocene-lower Oligocene transtensional rifting in the Bonaire Block opened of the Bonaire-Falcón basin causing the crystalline basement sequences of Aruba,Bonaire and Gran Roque to subside by ~ 1 km; Normal faults were inverted in the middle Miocene as the basin (Falcon, Bonaire) became transpressive [Gorney et al., 2007].

3. Methodology

The main objective of this research was the elaboration of two maps based in calculating the gravimetric response of 2 interfaces, basement-sediment, boundary between upper and lower crust through mathematical inversion.

The first step consisted in the compilation of the complete Bouguer anomaly (CBA) map, through the integration of existing data since 1976, for which a homologation of all the data had to be carried out [Araujo and Orihuela 2020]. We integrated 40,000 gravimetric stations on land. Offshore, satellite data was used [Sandwell et al., 2014]. The CBA values were elaborated at each measuring point by comparing the observed gravity value with a theoretical model based on the Geodetic Reference System (GRS80) and reduced to the surface, after free-air, Bouguer, and topography corrections were made using standard methods defined by LaFehr [1991]. Using a bandpass filter and eliminating low frequencies, a residual map of short wavelengths is obtained. The map associated with the basement-sediment interface was prepared from the information of wells that reach the igneous metamorphic basement and then by applying the Cordell and Henderson algorithm to the Bouguer residual map.

In the frequency domain we will use the approach of Spector and Grant, [1970], Mishra and Naidu, [1974]; Dimitriadis et al., [1987], which is based on the concept of power spectrum; when amplitude is on a logarithmic scale versus a linear scale for the frequency, there are intervals, where the slope of the tangent line to the curve is related to the depth of the source. The slope of the straightline is proportional to the depth to the top of the body. Thus, if k denotes the wavenumber and $S(k)$ the power spectrum, the depth d to the source can be estimated from the relation $S(k) = f(k)$, by employing the formula:

$$lnS(k) = -2kd \tag{1}$$

The gravity field values for a block of N × M equally spaced (windows) data are transformed from the space domain to the frequency domain by means of the 2-dimensional discrete Fast Fourier Transform. The N × M power spectrum are calculated and their associated depth d, these depths are assigned to the center of each window and then interpolated [Araujo, 2013].

3.1 Inversion of Cordell and Henderson

We apply a bandpass filter to the CBA, to obtain the residual anomaly map. Using the Cordell and Henderson [1973] inversion algorithm and the information from the wells that reach metamorphic igneous basement [Smith, 1980; Feo-Codecido et al., 1984], in the Apure Barinas, Falcón and Lake Maracaibo basins. A three-dimensional structural model (basement top) was calculated, automatically from gravity anomaly by successive approximations. A first approximation of structure is obtained by means of the Bouguer slab relationship. The gravity field of this first model is calculated and at each grid points the ratio of observed to calculate gravity is used to modify the first structural model, thus leading to a second approximation of structure. The process is repeated until the difference between the observed and calculated gravity is close to zero.

3.2 The radially averaged power spectrum of the complete Bouguer anomaly

The radially averaged power spectrum of the CBA was performed using Fourier transform and graphic the logarithm of energy in function of frequency [Spector and Grant, 1970]. From the slopes of this spectrum we estimate the depth to four major sources of gravimetric anomalies: Caribbean Plate, Mohorovic, the upper crust-lower crust boundary and the basement. Applying a bandpass filter to each of the mentioned intervals, we can produce a regional map (long wavelengths) and a residual map (short wavelengths). The calculation of the depth of the upper crust-lower crust boundary was made using spectral analysis applied to windows; square windows into which the study area is divided. These windows have a size that is approximately 5 times the depth of the source (100 km for upper lower crust boundary) that causes the anomaly, measuring the slope of each one of them, the depth is calculated and assigned to the center of the window, then through interpolation, a depth map of the interface is obtained [Spector and Grant, 1970, Mishra and Naidu, 1974; Dimitriadis et al., 1987; Narasimha et al., 1996; Araujo, 2013].

3.3 Euler deconvolution

Euler deconvolution [Thompson, 1982] is based on the application of Euler's homogeneity equation to a moving data window with SI (Structural Index) fixed at several tentative values. For each position of the moving data window, a linear system of equations is solved for the anomaly base level, and the horizontal (xo,yo) and vertical (zo) positions of the equivalent source. As a result, a "spray" of possible solutions is produced, each solution being associated with a moving data window position. Thompson [1982] presented a criterion to reduce the number of possible solutions and to estimate, at the same time, the structural index (for gravity data: SI = 0 indicates the assumption of a thin plate; SI = 0.5 contact, fault SI = 1, an elongated body; and SI = 2, a point source) [Reid et al.,1990; Thompson, 1982]. Resulting source points are always clustered, which describe edges of a body with density contrasts to their surroundings. Strong gradients in the fields lead to clustering in these specific areas that often belong to tectonic structures. In this investigation, the SI that correlated best with geological contacts and faults has a value of 0.5.

4. Results

The CBA range from 121 mGal to –121 mGal, with a mean of –30 mGal (Figure 2). The CBA reflects the lateral density contrasts associated with geological structures. The map shows the strong minimum in blue color (values between –170 to –26 mGal) with an SW-NE strike associated to Lake Maracaibo basin, and it is parallel to the strike of the Mérida Andes mountain range with an offset in northwestern direction of about 50 km (anomaly 1). In the case of an orogenic system in isostatic equilibrium, the minimum should coincide with the location of the mountain

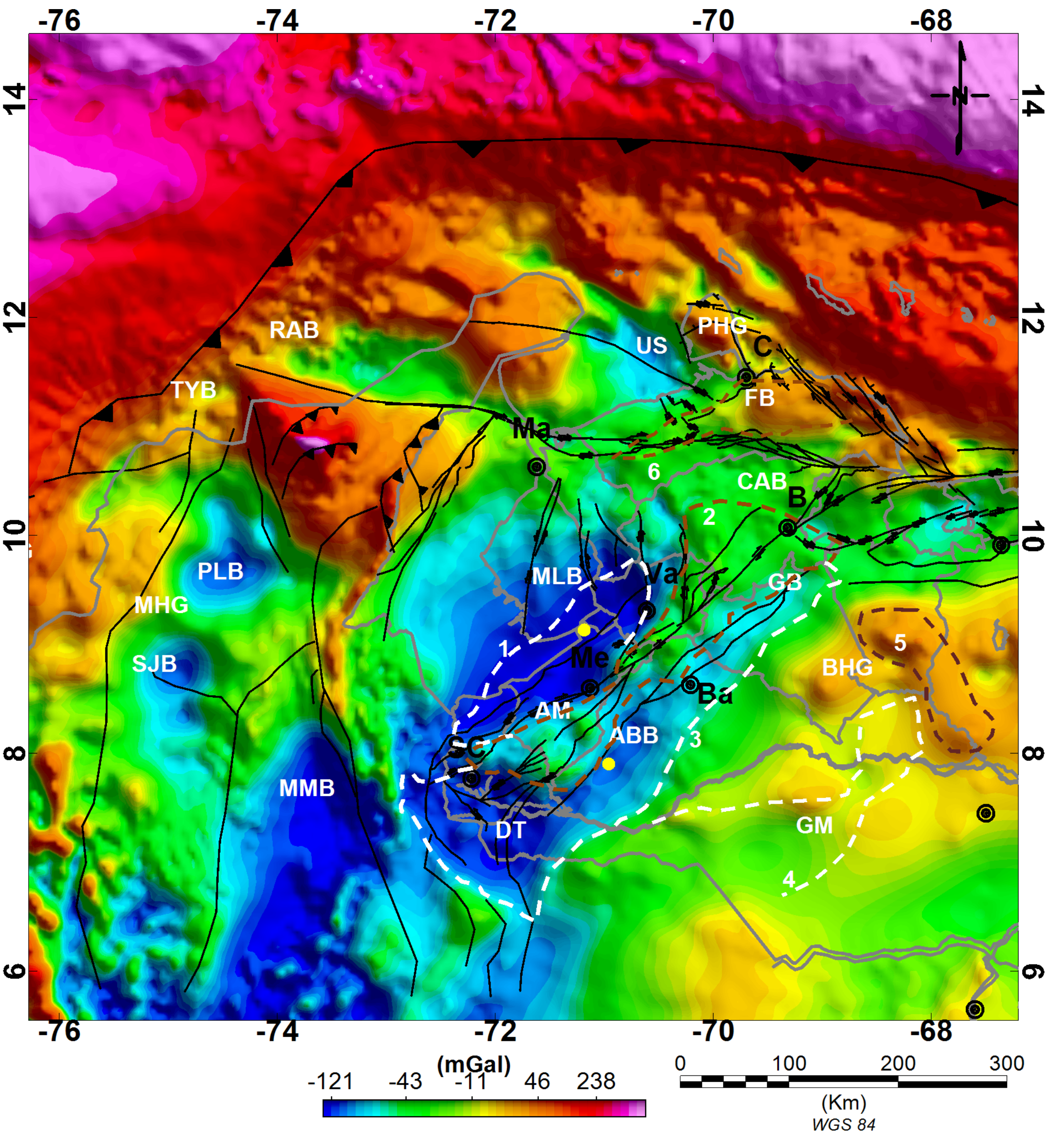

RAB	Ranchería sub basin	TYB	Tyrona sub basin	
PLB	Plato sub basin	MHG	Magangué basament high	
SJB	San Jorge sub basin	MLB	Maracaibo Lake Basin	
DT	Táchira Depression	MMB	Middle Magdalena Basin	strike-slip fault
ABB	Apure Barinas Basin	GB	Guarumen Basin	reverse fault
US	Urumaco Surco	PHG	Paraguaná high	
PGH	Paraguaná high	FB	Falcón Basin	normal fault
GM	Graben de Mantecal	BGH	Baúl high	

Figure 2. Complete Bouguer anomaly (CBA) map for western Venezuela and northwest Colombia, reduced with 2.67 g/cm^3. The white and brown segmented lines, numbered 1 to 6 represent gravimetric anomalies. Quaternary faults from Audemard et al. [2000]. Major geological provinces related to this study in white letters. Sources: Cediel et al., 2003; Ceron et al., 2007; Araujo and Orihuela, 2020. Ba = Barinas, B = Barquisimeto, C = Coro, Ma = Maracaibo Me = Merida, SC = San Cristóbal, Va = Valera. Yellow points represent center of gravimetric mínimum in the basins.

range. This minimum was originally associated to the large accumulation of sediments in the south of the Lake Maracaibo basin [Folinsbee, 1972], however, after several gravimetric modeling, different authors [Kellogg and Bonini, 1982; Escobar and Rodríguez, 1995; Arnaiz et al., 2011] concluded that this accumulation of sediments was not enough to produce the minimum; therefore, it was related with the configuration of different structures of long wavelength and at big depth. This minimum seems to be strongly controlled by the Boconó fault in the southern zone (see Figure 2), in fact this minimum ends abruptly against it. The Boconó fault, according to several studies [Estévez y Laffaille, 2010; Pérez y Mendoza, 1998, Audemard and Audemard 2002 Audemard et al., 2005] shows seismicity with an average depth of 15 km to 20 km along strike; to the Northeast the minimum is also delimited by the Valera fault, which presents an average seismicity in depth less than 15 km. Therefore, the gravimetric minimum is associated to geological structure with this depth range or to intra-crustal events. According to Audemard et al. [2005], most earthquakes in western Venezuela have a depth range between 2 and 40 km, which supposes an origin from fragile crust to ductile crust, [Audemard and Audemard 2002; Audemard et al., 2005]. If the gravimetric minimum is delimited by fault systems whose extension in depth does not exceed the lower crust, it can be inferred that the anomaly is caused mainly by sources at a depth of 20 to 30 km. In the CBA map (Figure 2), an anomaly with a range of −10 to −13 mGal, with a southwest-northeast orientation, is located about the Andean topography with a length of approximately 410 km from San Cristóbal to Barquisimeto, and an average width of 60 km (anomaly 2). In Figure 2 we can also see the minimum (−110 to −100 mGal) south of San Cristóbal which is associated with the Táchira depression where the basement is located approximately at 6 km depth (anomaly 3) [Feo Codecido et al., 1984]. This minimum covers part of the Apure basin and continues south of Barinas; here it is associated with the depression of Capitanejo (−75 to −85 mGal). At Barinas, the anomaly becomes less negative (−60 to −55 mGal), possibly associated with the Arch of Merida. Southeast of Barinas, the minimum not so prominent with values of −12 to −18 mGal (anomaly 4), which is a gravimetric response of the Mantecal graben; northeast of Barinas, two maxima are observed with 7 and 17 mGal, respectively, associated to Baúl high (anomaly 5). At south southeast of Coro shows a maximun (−10 to 30 mGal) with E-W strike which has an approximate extension of 200 km and an average width of 60 km associated with the Falcón anticlinorium (anomaly 6), this maximum would be mostly influenced by crustal shortening in this area [Bezada et al., 2008; Rodriguez and Souza, 2003]. The contribution of the upper mantle to the gravimetric anomaly is more than 60%, the expression of the sedimentary column is about 40 %.

4.1 Power spectrum

In the figure 3, the longest wavelength is related to wave numbers between 0 and 0.035 km^{-1}, which linked the gravimetric interpretation from the Caribbean plate, upper mantle (Mohorovic) and the middle crust, source between 0.035 until 0.075 km^{-1} is associated to upper crust and sediment. The intervals of the wave number 0.002 to 0.004 would be associated with Caribbean plate (average depth of 120 km) and 0.012 to 0.032 km^{-1} is related with intermediate sources corresponding to the limit between the upper crust and the lower crust (average depth of 20 km), the interval of 0.04 to 0.07 km^{-1} is associated to basement and the sedimentary column, with an average depth of 5 km.

4.2 Basement map

Based on the CBA residual map (Figure 4), and well information present in the western oil fields of Venezuela (we only have wells information in Venezuela) this map (Figure 5) was calibrated. Theoretically, this map represents the gravimetric anomaly caused by sources of the sedimentary column and the top of the metamorphic igneous basement. The long wavelengths have been suppressed and the short wavelengths have been enhanced, except the noise. From figure 5, the main structures are the Maracaibo lake depression with a maximum depth of the basement top of 10 km with a maximum sediment thickness of 5.0 km, to the north the Alto de Mérida, a structure with a strike perpendicular to the Andes, to the south Táchira depression with 6.5 km of sediment thickness, and the Mantecal Graben with 4 km of depth, the Surco de Urumaco has a depth of 6 km. East of the Apure-Barinas Basin, there is a contrast in the depths, associated with the limit between the Paleozoic and Precambrian basement; this contrast can be observed also in figures 2 and 4, the anomaly gradient is related with the Apure fault. In Colombia, the Tayrona and Rancheria basins show a depth of 8 km y 8.5 km, the Plato, San Jorge and middle Magdalena basins a depth of

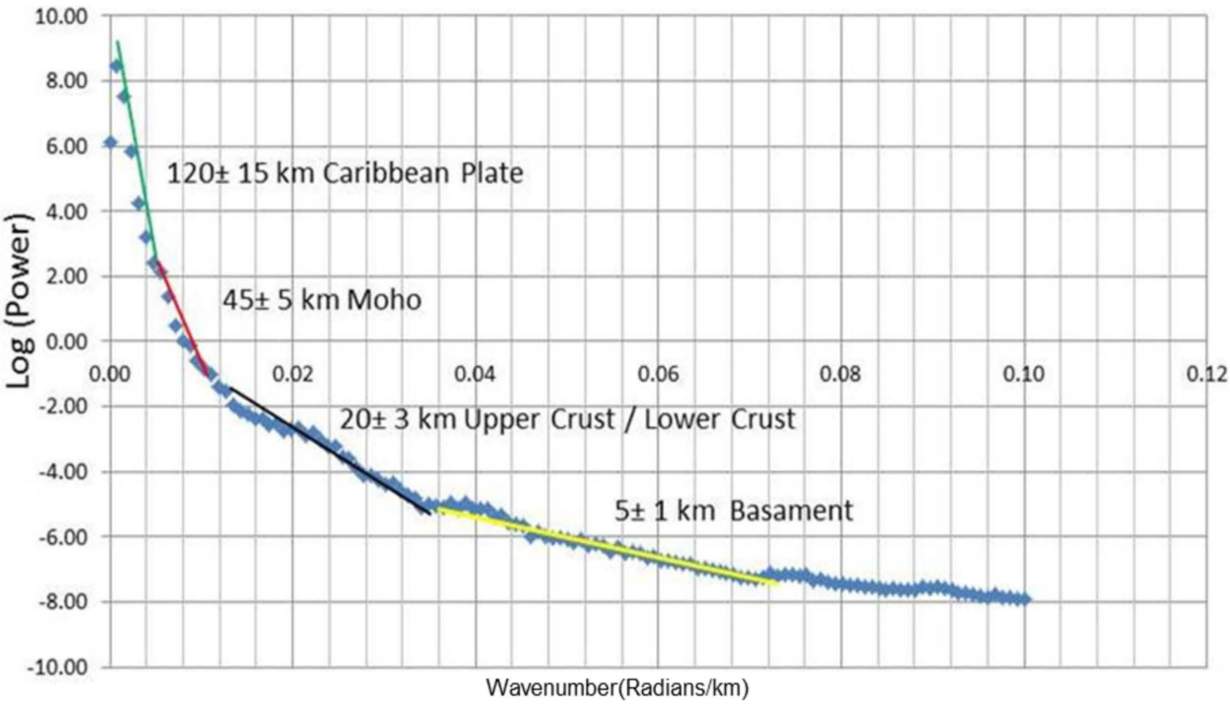

Figure 3. Radially averaged power spectrum of the CBA showing the source depths estimated from the slopes of the curve. The largest wavelength components are most likely associated with Caribbean plate and the Moho discontinuity, the mid wavelength component with the lower crust/upper crust boundary and, the shortest one, with the basement.

6.5, 5.5 and 7 km, respectively; theses values are in correspondence with values reported by Ceron et al. [2007]. To the south of Maracaibo basin, the sedimentation is controlled by the uplift of the basement. Figure 6 shows the good correlation between a reflection seismic line, wells and the depth of the top of basement obtained from the gravimetric anomaly (purple line).

4.3 Upper-lower crustal Interface

Figure 3 shows the spectral analysis of the CBA where depths of 17 to 23 km are associated with the upper-lower crustal boundary. This result with a certain margin of difference has been reported by various gravimetric studies [Arnaiz et al., 2011; Arnaiz and Audemard 2014; Cisneros 2016; Sánchez-Rojas, 2011; Sanchez-Rojas and Palma 2014; Linares 2015; García et al., 2009], it is evident that this depth is associated with a strong change in density. This contrast has been given little relevance in the results obtained by seismic refraction.

Using spectral analysis (as indicated in the methodology section) the map the interface between the upper/lower crust boundary (brittle and ductile shear zones) is obtained, and is associated to strong decoupling between the upper and lower crust, (in theory mainly affecting the Maracaibo block) this density contrast would be the cause of decollement that produces the uplift of the Mérida Andes orogen [Audemard and Audemard, 2002] along the westerns faults systems. These systems are mostly controlled by Bocono fault, Valera, Burro Negro, Burbusay, Hato Viejo, Caparo fault and northwestern and southeastern foothills faults. This discontinuity seems to be the limit seismogenic crust, since the seismicity observed in western Venezuela is located between the surface and 20 to 25 km depth [Monod et al., 2011; Audemard and Audemard, 2002] and it is also the depth where all the fault systems converge. In general, gravity minima over mountain ranges are related to isostatic compensation [Götze et al., 1995]; the gravimetric minimum associated with the Andean chain is delimited by the Bocono fault to the east and the Valera fault to the north, whose maximum depth does not exceed 22 km, in other words the root of the Andean chain is associated with this interface, while in the case of the Himalayas the detachment originates between the lower crust and the upper mantle according to Mattauer [1983, 1985], therefore there no isostatic compensation between

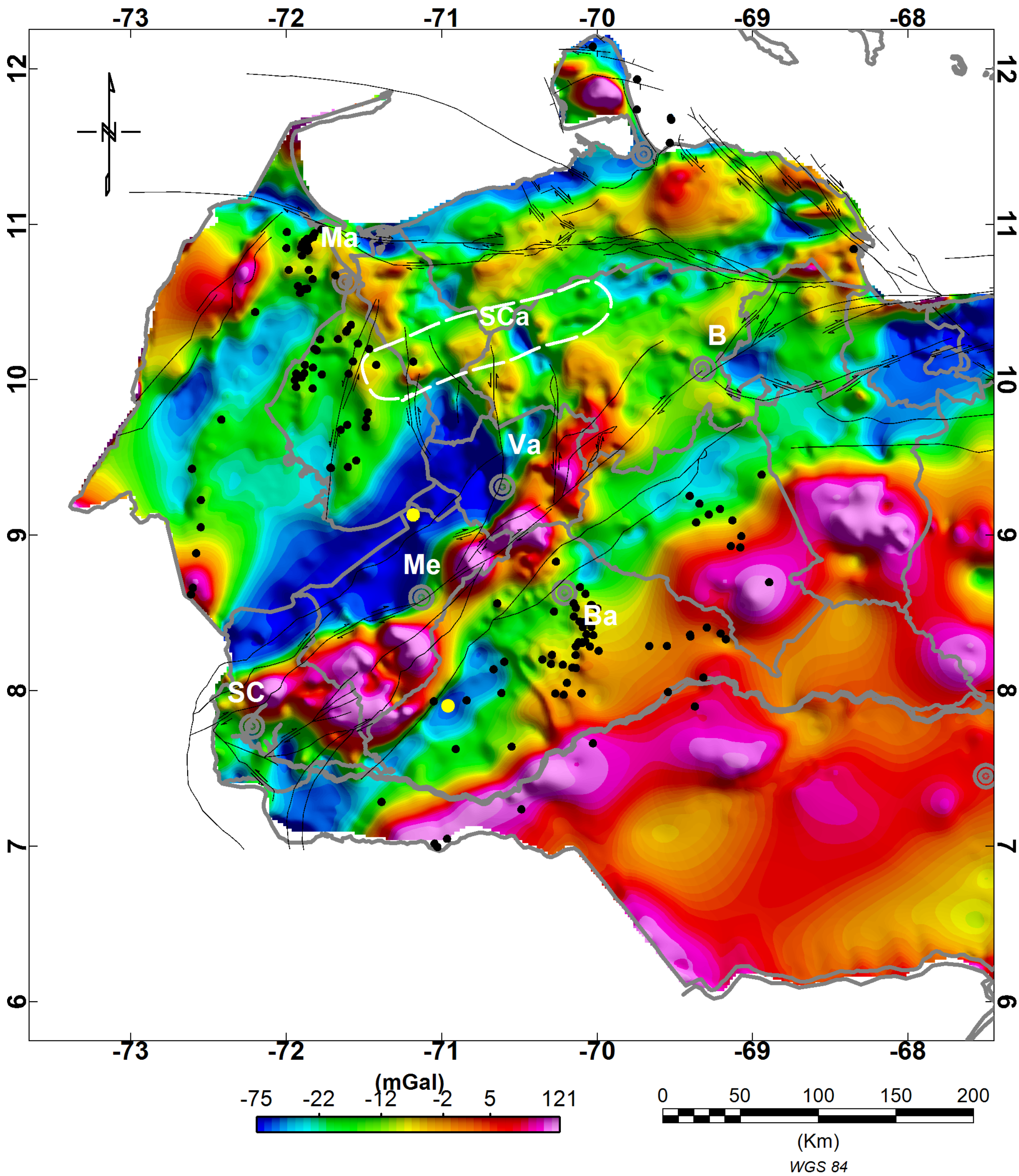

Figure 4. Residual map from filtering the short wavelengths of the complete Bouguer anomaly map. Gravimetric anomalies due to the density contrast in the upper crust and structures associated with the basement. The white line delimits the pattern of gravimetric maximum and minimum due to highs and lows in the basement topography. The minimum of −22 to −24 mGal corresponds to La Sabana de Carora (SCa), yellow dots represent the gravimetric minima in both basins. The black dots are the wells that reach the metamorphic igneous basement located in the oil basins of western Venezuela. Source: [Smith, 1980; Feo-Codecido et al., 1984].

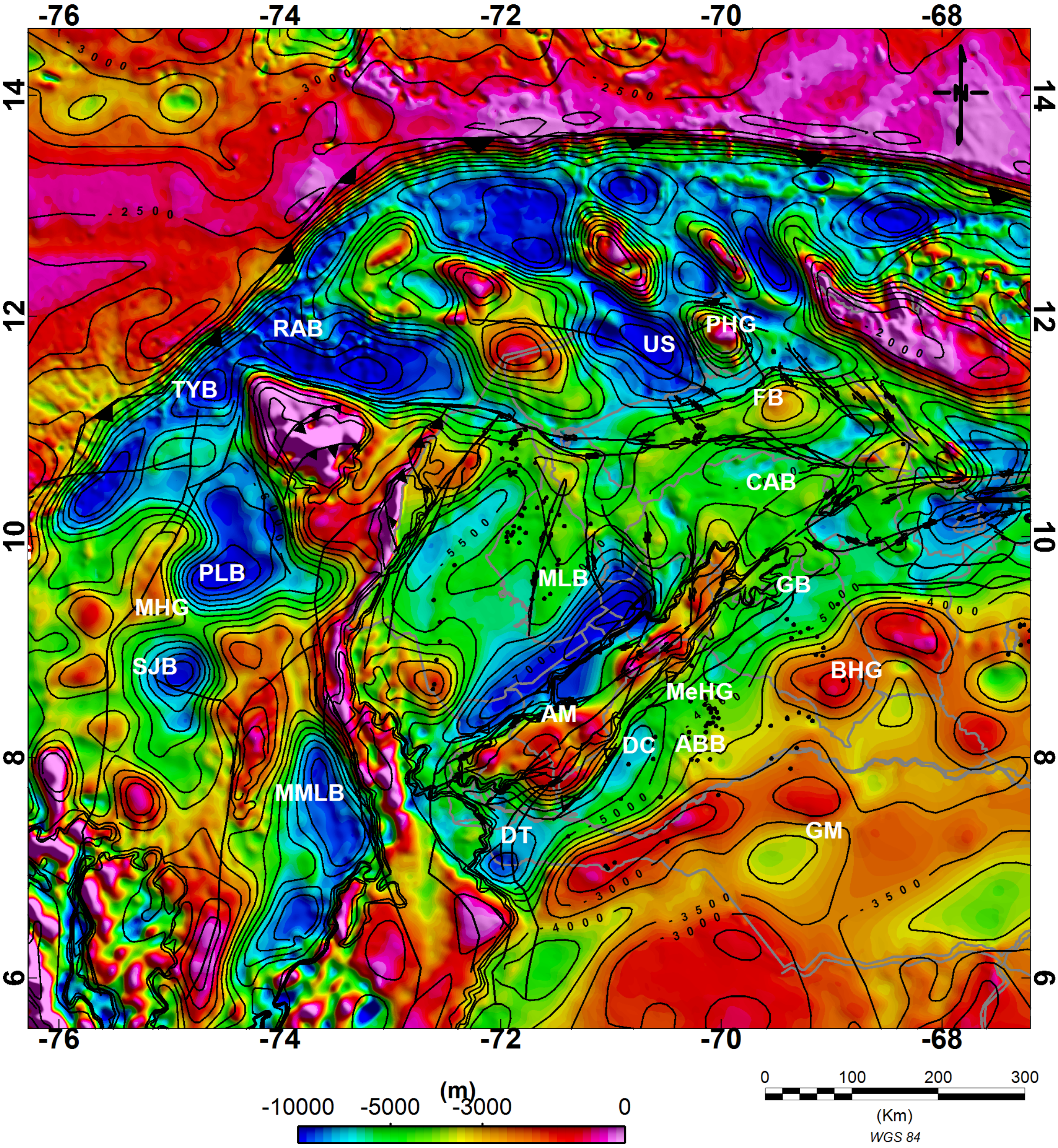

Figure 5. Basement map obtained from gravimetric inversion. Quaternary faults (black lines) from Audemard et al. [2000]. US = Surco de Urumaco, PHG = Paraguana high, FB = Falcon Basin, CAB = Carora Basin, MLB = Maracaibo Lake Basin, GB = Guarumen Basin, BHG = Baul high, MeHG = Merida high, ABB = Apure Barinas Basin, AM = Andes de Merida, GM = Graben de Mantecal, DT = Tachira Depression, DC = Capitanejo Depression, MMLB = Middle Magdalena Basin, SJB = San Jacinto Basin, MHG = Magangue Basament high, PLB = Plato Sub Basin. TYB = Tyrona Basin, RAB = Rancheria Sub Basin.

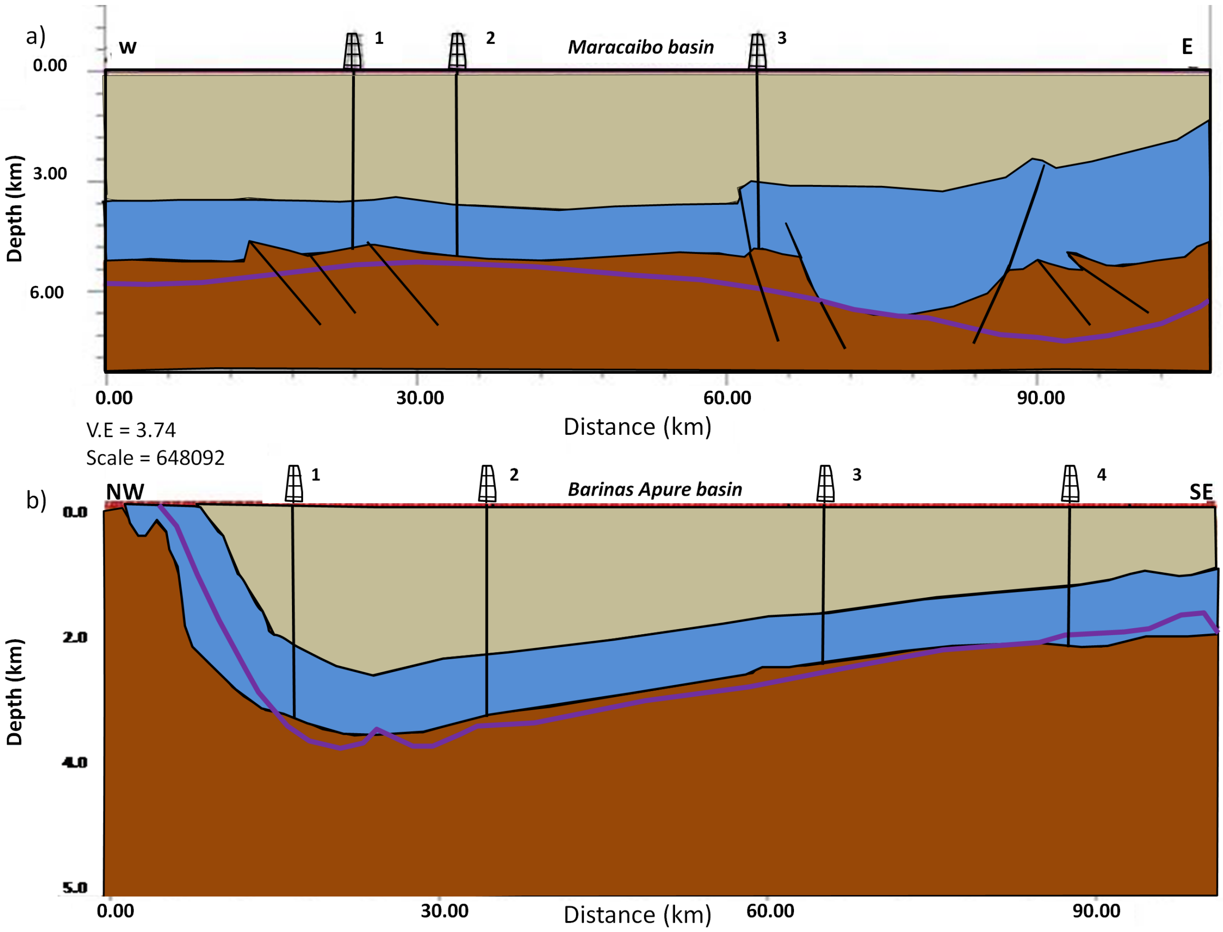

Figure 6. Comparison between the basement depth from gravimetric inversion (purple line) and the basement given by two seismic reflection lines (see figure 1 for the location of profiles 6a and 6b). The wells reach the metamorphic igneous basement located in Maracaibo Lake basin and Apure Barinas basin. Seismic line above [Escalona and Mann, 2003] below [Parnaud et al., 1995]

the mantle and the Andean chain. Isostatic compensation could be associated with the upper crust-lower crust boundary. The mountain range (Sierra la Culata) on the northwest side of the Boconó fault seems to be in isostatic compensation since the gravimetric minimum coincides with the topography and extends in the direction of the Valera fault, also the enormous accumulation of sediment in the basin the Maracaibo Lake, cause the displacement of this minimum in NW direction; consequently the Boconó fault is a limit of the physical properties, in this case the density of the Maracaibo block and the South American plate. Probably on the southeastern side, the Sierra Nevada is not isostatically compensated since the value of the CBA is not negative enough.

The CBA (Figure 2) presents a horse saddle shape on Merida city, of there, to the northeast, the Valera, Burbusay and Tuñame fault system seems to originate. The 1674 earthquake originated in this area [Palme et al., 2005] and there is a displacement deficit of 3.2 m that could give rise to an earthquake of considerable magnitude (>7) according to Pérez et al. [2011]; from the gravimetric point of view, a strong change in horizontal density from the southwestern Andes to the northeastern Andes is evident, which would cause the dispersion of the Boconó fault system, producing different branches of fault systems such as the Valera, Tuñame, Burbusay faults – these fault also delimit the block of Trujillo that is genetically related to the Caparo block to the south [Bermúdez, 2010] through the Uribante and San Lázaro graben [De Toni and Kellogg, 1993; Colleta et al., 1997; Lugo and Man, 1995], this block (Trujillo) presents an escape structure towards northeast by means of a detachment located between the upper and lower crust, according to Backé et al. [2006] and Donht et al. [2005], these two authors only infer the existence of this detachmet, but no proof is given for it. In this investigation we can observe the location and depth of this decollement (Figure 7).

From the map in figure 7, the depth of the fault traces including thrusts systems faults located on both flanks and strike-slip Bocono, Valera, Burbusay, Hato Viejo, Central-Sur Andino, Caparo fault systems is approximately the same (18 to 22 km), all these faults (strike slipe) belong to the Maracaibo block; Icotea fault system probably does not belong to this domain of faults that affect the Andean uplift. The Eastern Andean Front system fault of eastern mountain range of Colombia seems to have the same depths. According to Taboada et al. [2000] graben systems extended in a N-NE direction, from the Cordillera Real in Ecuador through the eastern cordillera of Colombia, one of the directions of these grabens is parallel to the Andes of Merida, so they could have common origin, which means, the mountain chain is the product of the inversion of Jurassic grabens such as the Uribante Graben to the south and the San Lazaro Graben to the north.

The other faults to the west (Santa Manta Bucaramanga, Palestina, Romeral and San Jacinto fault system) to the north (Oca-Ancon, Lagarto fault system) and to east (Apure, Altamira fault system) of Maracaibo block present a more pronounced expression of their traces (highest maximums) delimiting the domains of the blocks. It should be noted that due to the size of the window this filter is designed to calculate depths between a range of 12 to 24 km, (structures mostly associated with the Maracaibo block) for shallower or deeper sources, the depth values are not exact but the direction and strike of the structures are not affected, so they have a qualitative importance. In the west of the study area, the depths of the Santa Marta Bucaramanga fault system have a range of 17 to 19 km and a strike in northwest direction, while the Palestina and Romeral fault systems have a depth range of 18 to 22 km, with a strike in the north direction. To the north, the depths of the structures and traces of the faults (Lagarto, Rio Seco, Urumaco) have a range of 17 to 19 km and strike in a northwestern direction, the Oca Ancon fault system presents an abrupt density contrast (which can be associated with a domain change), and an east-west trend. The Morrocoy fault zone marks the northeast boundary of the North Andes plate with the Caribbean plate [Pérez et al., 1997; Bird, 2003; Pérez et al., 2018], this fault is the limit between different plates, Caribbean plate to the north, North Andean block to the west and the South American plate to the south. To the east of the study area, the depths of the Apure and Altamira faults have a range of 19 to 21 km and a strike in northeast direction, the high of El Baul show a depth of 17 to 19 km and a strike in northwest direction. In the central part, the fault systems associated with the Andean orogen has depths of 18 to 22 km and a strike in northeast direction. All these fault systems can be associated with a common origin with a depth range of 17 to 24 km.

4.4 Fault movements

There is some discrepancy reported by various authors regarding the magnitude of the dextral wrench offsets of the Bocono fault; Rod [1957] proposes 33 km, Alberding [1957] 65 km, Von der Osten and Zozaya [1957] 50 km, De Ratmiroff [1971] 75 km, Stephan [1982] 70 to 80 km; all these values are calculated due to the offset between outcrops, but erosion could affect the result. More recently, Escalona and Mann [2005] propose a displacement of 80 km based on the separation between Eocene deposits for the Apure Barinas basin and the Maracaibo Lake basin; Audemard and Audemard [2002] propose a displacement of 30 km based on the distance between gravimetric minima located in both flanks of the Andean chain (assuming that these minima coincide in the initial state); however, this measure refers to the maps generated by Bonini [1977], where at the time there was an error of 14.8 mGal for excess in some base points of the national gravimetric network [Orihuela, 2011] and on the other hand observing on the Bonini map there is not a good distribution of isolines to the southwest of Capitanejo, probably due to the fact that at this time no gravimetric surveys had been carried out in said area. In the new map of the CBA [Araujo 2014; Araujo and Orihuela, 2020] a minimum of substantial magnitude appears 30 km to the southwest of the Barinas city (Figure 2). This minimum is displaced 60 km towards SE with respect to the minimum corresponding to the Lake Maracaibo basin. This value would be close to the one proposed by Alberding [1957], where he calculates the offset between precambrian outcrops. Observing the geological map of Hackley et al. [2006], there is a separation of approximately 60 km for the geological bodies of Tostos Asociacion (Pzut) belonging to the Upper Paleozoic and the same offset for Cretaceous outcrops located southwest and northeast of Merida city. Also, from figure 7 (white lines) and figure 4 (Andean orogen structures adjacent to gravimetric lows – see the yellow dots), we can see the displacement between two structures on the left and right side of the Bocono fault is 60 to 65 km, this offset is caused by the right lateral displacement of the Bocono fault. The Santa Marta Bucaramanga system fault (SMBF) limits the west side of the Maracaibo block, observing the figure 7 we can see the trace associated to the gravimetric maximums, the left strike slip displacement was calculated for two structures, these two structures were chosen

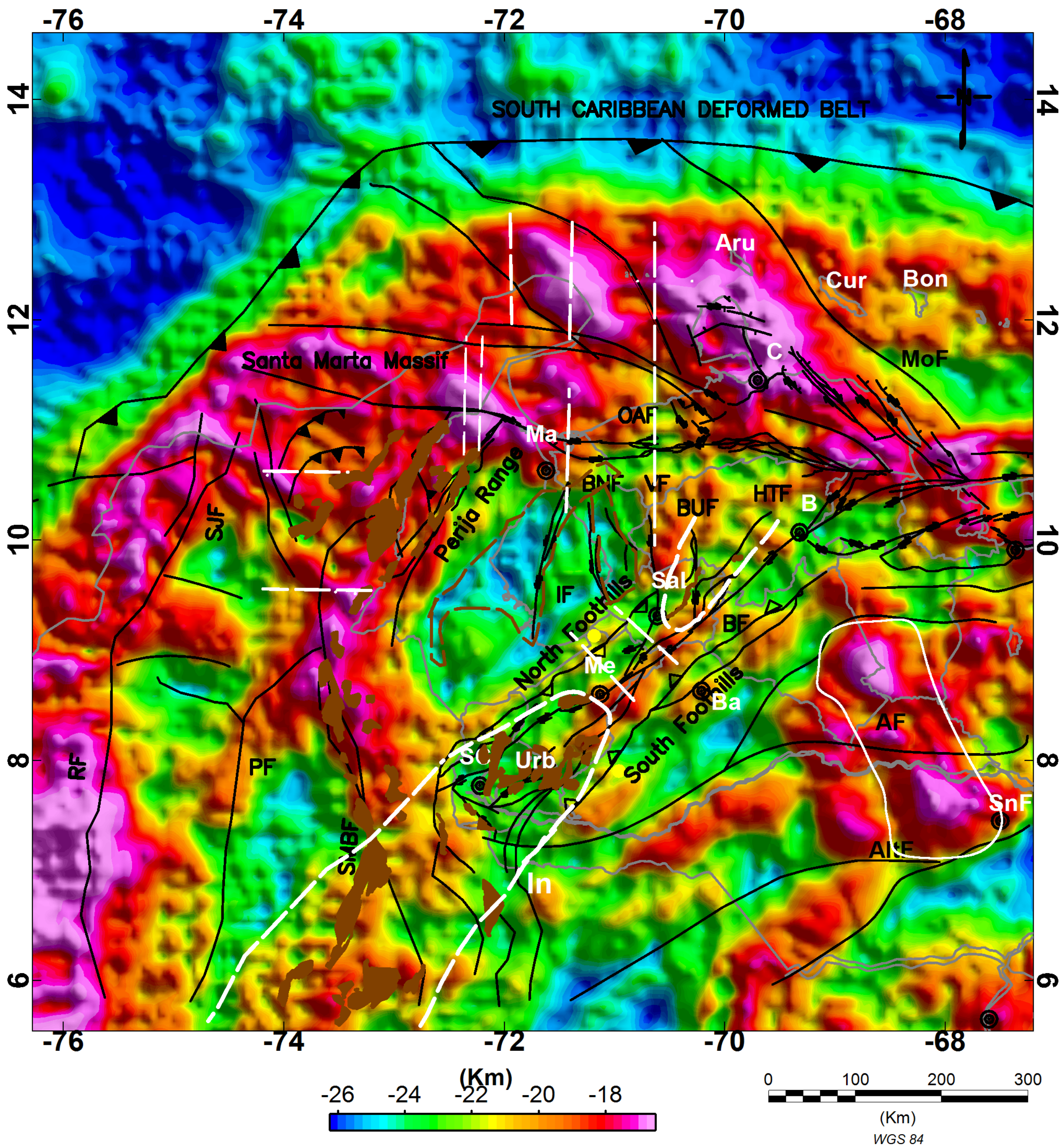

Figure 7. Map of upper-lower crustal boundary. The maximums (red and violet color) can be associated to fault systems in western Venezuela and northern Colombia. The fault systems associated to Mérida Andes present a depth of 18 and 23 km. White letters represent cities SC = San Cristobal, Me = Merida, SaL = San Lazaro, B = Barquisimeto, Ba = Barinas, C = Coro, Ma = Maracaibo, Urb = Uribante (Pregonero), Aru = Aruba, Cur = Curacao, Bon = Bonaire. Interpreted faults MoF = Morrocoy fault, AltF = Altamira fault. White solid line represents the strike of El Baúl Massif. North-south dotted white line represent to the trace that lines up with, the Peninsula de la Guajira, Icotea, Pueblo Viejo fault, Surco de Urumaco, Peninsula de Paraguana. Curved dotted white line represent Jurassic grabens such as the San Lazaro Graben to the north, (the line to the west of the graben would be associated with paleo Valera fault) and the Uribante Graben to the south. The white parallel line in the central part of the Mérida Andes and Santander Massif represent the distance between structures associated with the displacement of Bocono and Santa Marta Bucaramanga fault. Grey line political division, brown dotted area = outcrops, Jurassic La Quinta formation.

(it is assumed that for a previous time they were united) because they have the same strike and magnitude. The black lines are drawn on the maximum, resulting in a displacement about 110 km, value according to those found by Kellogg [1984].

4.5 Block movements

The Bonaire Block has subsequently been entrained within the south Caribbean Plate margin and has been deformed by dextral displacement between the Caribbean and South American plates. These displacements involve the Oca Ancon fault system (Figure 7). In the following discussion, we will explain how the velocity of the plateau of the Caribbean plate is different from the velocity of the of Bonaire block.

The movement of Bonaire Block from its position near the Guajira peninsula since the Palecocene [e.g. Pindell et al., 2009; Wright and Wild, 2011; Urbani et al., 2013] also involves the movement of the Oca Ancon fault from the late Paleocene (ca. 59 Ma). Some authors propose an eastward translation of at least 300 km for the island of Bonaire relative to Guajira [Priem et al., 1986, Urbani and Grande 2013; Wright and Wild 2011]. But the displacement of this fault is not 300 km, Kellogg [1984] calculated 98 km, Vasquez and Dickey [1972] calculated 70 km, Tschanz [1974] 50 km. In figure 8, r_1 represents the distance between the Guajira Peninsula (origin) and Morrocoy fault or Curacao island, r_2 distance between origin and Bonaire island, r_{O1} is the displacement of Oca Ancon fault, r_{O2} displacement Bonaire block, r_{1O} and r_{2O} is the displacement of Curacao, Bonaire island respect to Oca Ancon fault, $r_1 = r_{O1} + r_{1O}$; $r_2 = r_{O2} + r_{2O}$ the velocity of Oca Ancon fault is $V_{Ocaf} = (r_2 - r_1)/\Delta t = \frac{(r_{O2} - r_{O1} + r_{2O} - r_{1O})}{\Delta t}$ assuming that both islands move with the same velocity for the same time with respect to the Oca Ancon fault, it is possible to make the approximation that r_{1O} is equal to r_{2O}, $(r_2 - r_1)/\Delta t = \frac{(r_{O2} - r_{O1})}{\Delta t}$ $V_2 = r_2/\Delta t = 400/59 = 6.77$ mm/yr; $V_1 = r_1/\Delta t = 300/59 = 5{,}084$ mm/yr; $V_{Ocaf} = (V_2 - V_1) = 1{,}69$ mm/yr, from figure 8, the velocity of Oca Ancon fault is approximately 1,695 mm/yr, a value that agrees with the value calculated by Audemard 1996 (1.88 + 3 mm/yr) and Soulas 1987 (1.65 + 0.35 mm/yr), the value of the displacement of the Oca Ancon fault from 59 million years ago

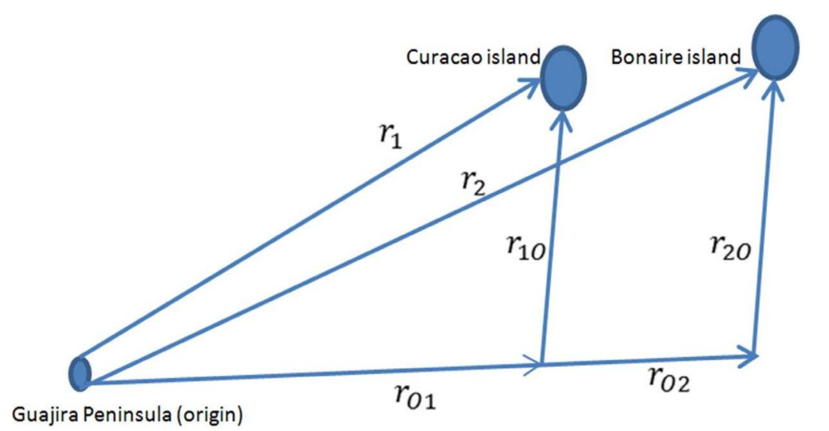

$r_1 = r_{01} + r_{10} \qquad r_2 = r_{02} + r_{20}$

r_1 = *Displacement of Curacao Island*
r_2 = *Displacement of Bonaire Island*
r_{01} = *Displacement of Oca Ancon fault*
r_{02} = *Displacement of Bonaire block*
r_{10} = *Displacement of Curacao island respect to Oca Ancon fault*
r_{20} = *Displacement of Bonaire island respect to Oca Ancon fault*

Figure 8. Vector diagram associated with the movement of the Oca Ancon fault, Aruba Bonaire Island and the Bonaire block. The r_1 represents the distance between the Guajira Peninsula (origin) and Morrocoy fault or Curacao island, r_2 distance between origin and Bonaire island, r_{O1} is the displacement of Oca Ancon faut, r_{O2} displacement of Bonaire block, r_{1O} and r_{2O} is the displacement of Curacao, Bonaire respect to Oca Ancon fault.

would be, r_{O1} = 100 km, value that is in agreement with that proposed by Kellog et al. [1984], and with that found by Laubscher et al. [1987] who estimate by means of a kinematic analysis that the displacement value of 100 km for the offset of the Oca Ancon, 110 km for Santa Marta Bucaramanga fault and 60 km of displacement Bocono fault.

The velocity of 5 mm/yr is an average value associated to the western part of the Bonaire block (west of the Morrocoy fault) and not to the reported value of 19 mm/yr of the Caribbean plate [Pérez et al., 2018; 2010; Trenkamp et al., 2002]. If we align the traces of the different structures that are generated by the movement of the Caribbean plate inside the Bonaire block with the direction of the strike of the main faults of Jurassic origin (Icotea, Pueblo Viejo and Valera) through white north-south lines (Figure 7). We can perform the following calculations, for example, there are 60km displacement measured from the origin Peninsula de la Guajira in direction east west to the first trace that lines up with the Icotea fault, would correspond to a formation time of 60/5 = 12 Ma, but the correct time is 59 Ma minus 12 Ma, is equal to 47 Ma, which is the reactivation time (in strike slip) in the early Eocene of the Icotea fault, said value coincides with the one published by Escalona and Man [2003b], Lugo and Mann [1995], following the same reasoning the reactivation value of the Pueblo Viejo fault gives us a value of 42 Ma that corresponds to the reactivation of the late Eocene value reported in Escalona and Mann [2005], the Surco de Urumaco has a distance of 145 km from origin, therefore the time is (59 – 145/5) = 30 Ma. According to Baquero [2015] proposes that the formation of the Surco de Urumaco is Oligocene, which would be in accordance with the value found, likewise, there is a distance from the origin to the alignment of the Paraguana peninsula with the basalt intrusions to the south of the Falcon Basin(central falcon) which is 195 km, which gives us a time of (59 – 195/5) = 20 Ma, which is between the range of values reported by Baquero [2015], Muessing [1978], Mcmahon [2000], the values associated with the intrusion time decrease from west to east according to the change of the Caribbean plate and in this case to the movement of the Bonaire block. Therefore, there must be a mechanical coupling between the Caribbean plate and the Maracaibo block.

4.6 Evidences for block movements from Apatite fission track (AFT) data

The paleo Valera fault (west fault of San Lazaro Graben) would be aligned with the trace that is 145 km away from the origin (Figure 7), which represents a time of (59 – 145/5) = 30 Ma, or early Oligocene time. This rank (30 to 36 Ma) is reported by Kohn et al. [1984], Bermudez et al. [2010] and it is associated with the first pulses of the Andean uplift reflected through the granite of Valera, figure 9A represents the Oligocene uplift associated with the interaction of the Caribbean plate (to the north) and not with collision of the Panama arc, since it started in the middle Miocene (15-12 Ma) [Bermudez et al., 2010, Montes et al., 2005]. This interaction could have caused the activation in sinistral strike slip with a vertical component of the normal faults associated with the opening event of the Jurassic. According to James [1990] to the southwest of Valera the fault splays westward as a series of north or south yielding thrusts that transform the sinistral movement and resolve the space problem created where a southward moving block, west of the Valera fault, meets a northeastward moving block on the northwestern side of the dextral Bocono fault. This configuration could have created the uplift of the Valera granite in the southern part of the paleo fault, although the Bocono fault is not active at that time but there is a block that interrupts the continuity of the paleo fault. In the figure 9A for this time an elongated graben is observed which contains the San Lazaro Graben to the north and Uribante Graben to the south, the coordinates of the AFT (Apatite fission track) values were displaced 60 km in a southwest direction to eliminate the right lateral displacement of the Bocono fault for this time. Figure 9B represent Miocene to Pliocene time, the Andean uplift is produced by the strain in a northwest-southeast direction due to the rotation of the Maracaibo block, the separation between the two grabens begins, Jurassic outcrops are widespread in the Merida Andes (Figure 7, doted brown color) Jurassic red beds usually belong to inverted grabens, the border faults of which being reactivated as regional high angle strike slip faults. To compensate compression strain, new neogene low angle thrust faults are produced [Colleta et al., 1997] the traces of the thrust faults are parallel to the faults of the main grabens, these faults have a low angle which have a decollement at level limit between upper and lower crust (Figure 7). Figure 9C shows the current configuration of the Andean chain and the AFT values taken from Bermudez et al. [2010]. During the late Miocene to early Pliocene, oblique convergence between the Maracaibo block and the South American plate was enhanced by collision of the Panamá arc with South America [Pindell and Kennan, 2001; Montes et al., 2005]. The oblique movement of individual tectonic blocks in the Venezuelan Andes along the Boconó fault system, during phases of transpression, appears to have controlled the timing of rapid exhumation by creating topography [Bermudez et al., 2010]. It can also be seen in

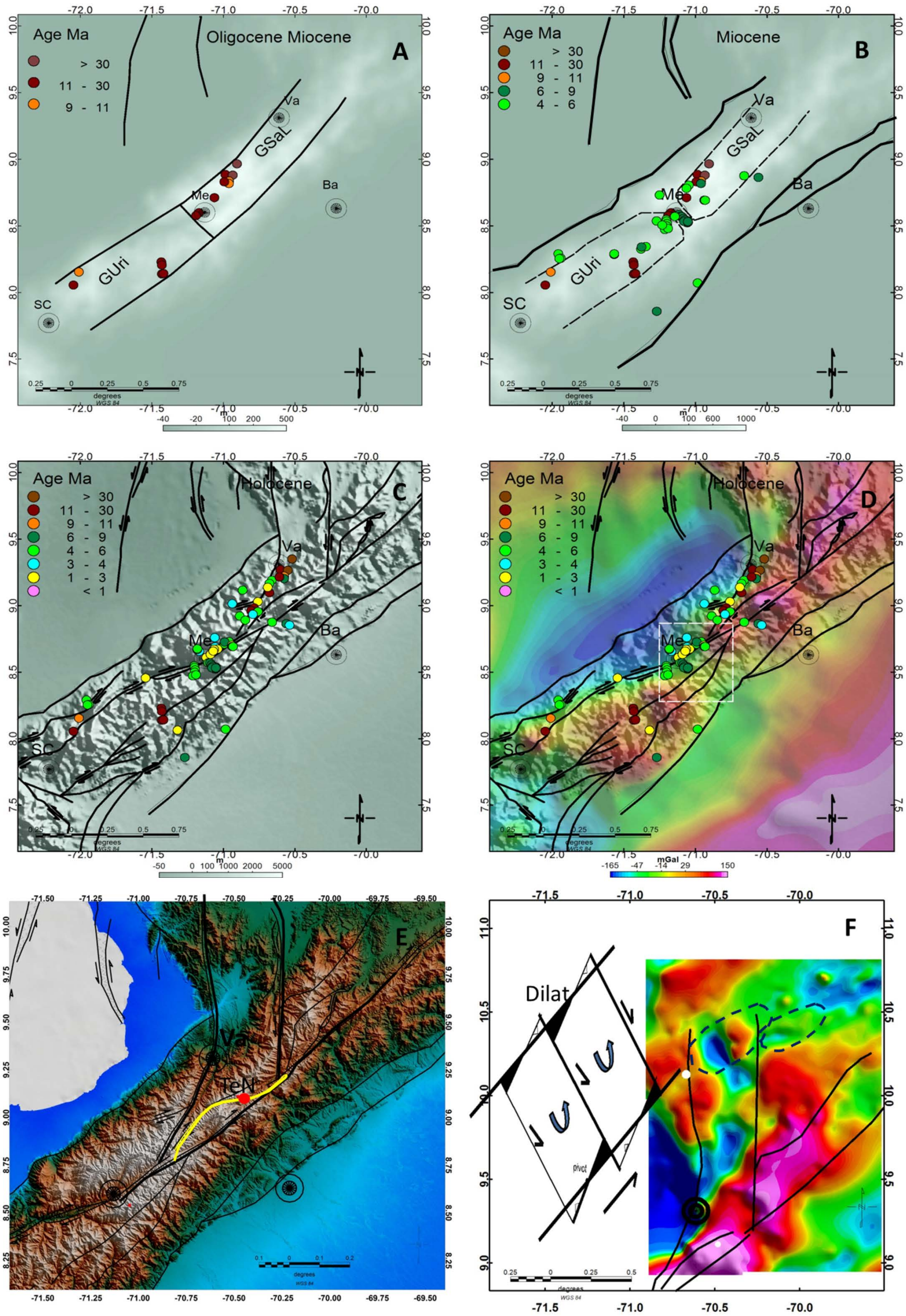

Figure 9. AFT (Apatite Fission Track) data taken and modified from Bermúdez et al., 2010. For figure 9A and B The location of the outcrop samples in the figure was made by eliminating the 60 km right lateral displacement of the Bocono fault. Figure 9A shows the values AFT corresponding to the Oligocene and the probable location of the San Lazaro and Uribante Grabens. Figure 9B shows the appearance of the low angle traces associated with the thrusts fault for the Miocene 9 to 4 Ma. Figure 9C is the current configuration of the Andes. Figure 9D is the current configuration and the CBA where the youngest AFT values correspond to the interval associated with the displacement of the Bocono fault, box in white. Figure 9E, the yellow line shows the configuration associated with the structures that originate in the southern area of the Trujillo block, the pivot point in red color is the central zone which coincides with the Teta de Niquitao, the highest topography area of Trujillo. Figure 9F the gravimetric map show high and low gravity values in the Tuñame wedge and conjugate expression in the north of the Valera and Burbusay faults, with a northwestern basin and a high to the north-east as the model is proposed to the west of the figure, the white point is the location of El Baño granite. Black letters represent cities SC = San Cristobal, Me = Merida, Va = Valera, Ba = Barinas, GSaL = San Lazaro Graben, GUri = Uribante Graben.

figure 9D how the most recent AFT values could be associated with the right lateral displacement of the Bocono fault (values inside the white square; this square coincides with the area where the greatest displacement Bocono fault occurs); therefore, Boconó fault could also deploy vertical offset [Schubert, 1982; Giegengack, 1984]. The San Lazaro Graben bounded on the west by the Valera fault and on the east by the Burbusay fault, seems to be shifted and rotated in the counterclockwise direction, between Miocene to Holocene time, there is a 30 degree rotation figure 9B, C of the Valera fault and Burbusay generating individualizing two triangular wedges (Tuñame and Burbusay wedges) this rotation is due to the displacement of the Bocono fault. If R equal to 38 km is the radius of a circle centered on the Valera fault and its limit is the Burbusay fault, the displacement due to rotation is given by $R\theta = \Delta x$, $\Delta x = 22$ km, the average AFT for samples associated with the range of 1 to 3 is 2Ma, figure 9C. Measurements from two samples south of Valera granite possibly associated with this rotational event imply a velocity of 22/2 equal to 11 mm/yr. When the displacement was about 40 km due to their vertical component exhume rocks whose average AFT value is 3.5 Ma (Figure 9C, 9D, the 40 km displacement is measured from the center of the white box) which implies a velocity of 11.5 mm/yr. Offset of Quaternary features along the fault trace yields a Quaternary slip rate between 3 and 14 mm/yr and 14 and 18 mm/yr [Schubert,1982; Audemard et al., 1999, 2000], These values are supported by the 11 mm/yr derived from the GPS data [Pérez et al., 2001]. For a velocity range between 11 to 14 mm/yr corresponding to the offset rate in the central zone of the Andes would give activation time about 4 to 5 ma for Bocono fault (taking 60 km as displacement). Beck et al. [2006] did not find evidence of on-going uplift in the area of study (Trujillo block), suggesting that the present-day high topography is minimal compared to the elevation acquired by the end of the Mio-Pliocene, which enhances the fact that the displacement of Bocono fault had to have started between 4 to 5 ma. Figure 9 E shows Tuñame wedge, where there is high topography to the south of the yellow line (this line almost coincides with the Tuñame fault) and low topography to the north, the pivot point (in red) is the central zone of the Tuñame wedge, which coincides with the Teta de Niquitao, this point has the highest topography in the northeastern Andes. In figure 9F the gravimetric map show high values in southwest and low values in northeast and conjugate expression in the north of the Valera and Burbusay faults, with a northwestern basin and a high to the northeast, west cartoon shows the tectonic configuration for a rigid block under the domain of parallel strike slip faults. This system rotates in counterclockwise direction.

4.7 Euler deconvolution

Figure 10 shows the good correlation between Euler's solutions and the quaternary fault system, with values ranging from 5 to 20 km (red and green colors) being the most dominant, this range is associated with the fault systems located in the Andes (Bocono, Valera, Caparo, Burbusay, and the thrust faults on both flanks) these values would be related to the upper and lower crust, this would be one more proof that the fault system has Its origin in the Conrad discontinuity, the Apure fault shows a depth that involves the entire crust (20-40 km, sky blue and blue colors).

5. Discussion

Between the Apure Barinas and Lake Maracaibo basins a considerable asymmetry in CBA minima is observed; this is caused by the different for both sedimentary thickness; the enormous accumulation of sediments in the basin of the Lake Maracaibo is associated with high production of hydrocarbons, being less the production of the Apure Barinas basin [James, 2000].The depths of the basement in the basin of Lake Maracaibo is high to the south and decreases towards the north, which is typical of a basin that originates from flexure of the lithosphere. The Mérida high and Baúl high are structures with a strike perpendicular to the strike of the Andes. The The Baúl high interrupts the continuation to the north of the Mantecal graben, in the same way it cuts off the continuation of the Espino graben to the south; therefore, this structure would be important in oil exploration.

In the north, the Oca-Ancon fault marks a structural domain change which depends on the relationship between the Oca Ancon fault to the south and the south Caribbean deformed belt to the north, the structures have a strike in east-west to northwest-southeast direction and all faults converge to the Oca Anacon and the Cuiza faults, the lateral strike slip of these faults would be associated with the different pull-apart basins offshore (Surco de Urumaco, Aruba, West Curacao, and East Curacao basin) according to Muessing [1984], Macellari [1995] and Gorney et al. [2007].

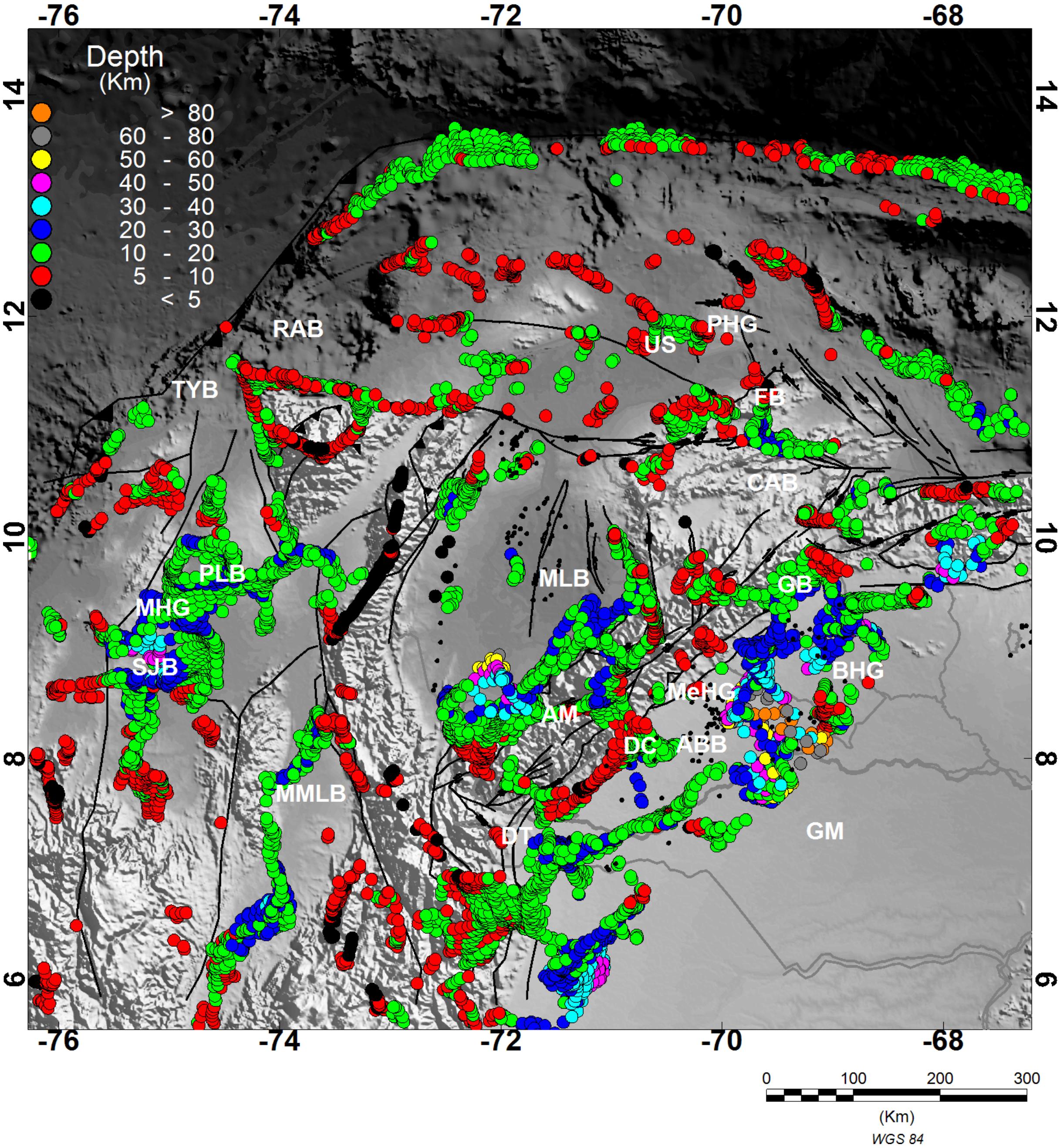

Figure 10. Euler deconvolution in western Venezuela and northern Colombia, the range of depths goes from 5 km to greater than 80 km, with red (5-10 km depth) and green (10-20 km depth) being the dominant depth ranges.

The tectonic phase during the early-middle Miocene, and still active locally, is characterized by rifting of the east-west-trending Leeward Antilles ridge along northwest-striking normal faults [Gorney et al., 2007]. However these faults according to figure 7 should have a strike slip component, since these are originated due to the relative movement between the Oca Ancon fault to the south and the South Caribbean deformed belt to the north. The distance about 300 km between the fault that cuts the Guajira peninsula and the Morrocoy fault, presents same gravimetric characteristics (gravimetric heights, strike directions) associated with the north domain, which change to east of the Morrocoy fault, this domain would be related with the translation of Bonaire island from the peninsula, this distance (300 km) is proposed by different authors [Priem et al., 1986; Urbani and Grande, 2013; Wright and Wild, 2011] for the eastward translation of Soebi Blanco Formation located on the island of Bonaire and were interpreted to possibly derive from the basement of today's Guajira-Santa Marta regions of Colombia. The pull-apart model proposed by Muessing [1984], the author evokes two models for basin formation, 300 km and 150 km of dextral displacement between the south Caribbean deformed belt and Oca Ancon fault system, the author opts for model where it is only 150 km necessary for the formation of the different basins, but in attention to previously mentioned, the displacement would be 300 km. This domain is related to the existing movement between the Oca Ancon fault and the southern Caribbean deformed belt, which originates pull apart basins north of the Oca Ancon system fault.

In the eastern domain (Figure 7) there is the Apure fault which according to Feo Codecido et al. [1984] marks the change of domain from Paleozoic to Precambrian basement; it also branches in a northeast direction near the of Barinas city and continued in east west direction, to the south we probably have the Altamira fault that limits the Mantecal Graben. The expression of El Baul Massif (in red color) is very well defined in a northwest-southeast direction, the magnitude of the depth and the direction of the strike indicate that this structure would not be associated with the Andean system. According to Mazuera et al. [2019], El Baúl Massif has seismic characteristics more similar to the Proterozoic basement than the Mérida Andes. According to the map, this structure seems to be aligned with the maximum of the Paraguana península, according to Baquero [2015] the new Permian ages obtained in the basement of northwestern Venezuela are compatible to those reported in the Paraguaná peninsula, Santa Marta massif 2010.

The Santa Marta Bucaramanga fault (SMBF) limits the western side of the Maracaibo block, The continuation of the strike-slip fault system has even been put in doubt by Ujueta [2003] who suggests the SMBF to consist of two completely different faults. The Santa Marta and the Bucaramanga faults respectively, there is no real surface expression of faulting in the vast alluvial cover of the 100 km wide Cesar valley nor did there seem to exist until recently firm seismic or gravimetric evidence of a vertical fault structure existing in the subsurface of the Cesar-Ranchería valley [Diederix et al., 2020]. However, recent work by Mora and Garcia [2006] mention that reprocessing and re-interpretation of existing subsurface seismic data has led to the confirmation of the existence of a vertical fault structure that follows the lineament of the projected central segment of the Bucaramanga fault that crosses the Cesar valley, but they consider that it must be a strike-slip fault structure of low level activity [Diederix et al., 2020]. Observing the figure 7 we can see the continuation of the trace associated with the gravimetric maximums, from the figure the left strike slip displacement was also calculated for two structures on both sides of the fault (distance between two line white) resulting in about 110 km of separation value according to those found by Kellogg [1984], Boinet et al. [1989], Laubscher [1987] and Mora et al. [2017].

The change in direction of the strike of the structures associated with the Colombian and Venezuelan Andes would be given by the indenter of Pamplona [Boinet et al., 1985] (marked within Figure 7) which, according to Ellis et al. [1996], is associated with the collision between two plates, one more rigid and the other weaker, the most rigid block in this case corresponds to the shield of Guyana and Maracaibo block corresponding to the weaker block. The indenter of Pamplona according to Audemard and Audemard [2002], causes the left and right dextral movement of the Santa Marta Bucaramanga and Bocono faults and therefore the escape of the Maracaibo block. According to Audemard and Audemard [2002] the Pamplona indenter verges westward, as attested by the left-lateral slip of the Bramon-Chucarima-Pamplona fault system on the northeastern side of the Santander Massif. The structure of the Táchira Depression can be explained as the consequence of the relative movements of two rigid blocks, Merida Andes to the northeast and the Cordillera Oriental of Colombia to the southwest, separated by a thick sedimentary pile which absorbed most of the stresses produced by the movement of these two blocks [Macellari et al., 1984]. Therefore, the Táchira Depression is caused by the relative movement of these two blocks produced by Pamplona Indenter.

The movement of Trujillo block is a consequence of a void effect induced by a bookshelf rotation mechanism produced by simple shear between the Oca Ancon and Bocono faults this mechanism is the cause of the Tuñame fault [Audemard et al., 2005]. This rotational movement, as previously stated (block movement section), originated at a time of 2-3 Ma which would agree with the formation time of the Tuñame fault, which, according to Schubert and Valastro [1980], is of Pleistocene age. Therefore it is unlikely that the activation of the Bocono fault strike slip started at the same time as the formation of the Tuñame fault. In the figure 9A and B the location outcrop samples was made correcting the 60 km of displacement right of the Bocono fault. Figure 9A shows the values (AFT) corresponding to the Oligocene and the probable location of the San Lazaro and Uribante Grabens. Figure 9B shows the appearance of the low angle traces associated with the fault thrusts for the Miocene time between 9 to 4 Ma ago and the beginning of the separation of the grabens, product of the start of the displacement of the Bocono fault probably from 5 to 4 Ma ago. Figure 9C shows the current configuration of the Andes, the dots in yellow color range ages 1 to 3 Ma which are aligned with the strike slip Bocono and Valera fault. Figure 9D shows the CBA where the youngest AFT values correspond to the interval associated with the displacement of the Bocono fault (white box). The uplift of the Andean mountain range was possibly dominated mainly by the northwest-southeast compression until 4 Ma ago, then in the Pleistocene time the displacement of the Bocono fault and the rotation of the Trujillo block began to control the current structural configuration of the northeastern Andes. The rotation of blocks near the intersection of the Bocono and Valera faults, cause incompatible motion at the corners of blocks and leads to the development of normal and reverse fault segments. In the south-east corner of the Trujillo block, the reverse faults originate due to the thrust fault; on the northeast side the normal faults occur due to the tension caused by the movement to the north (Figure 9E, F). This stress configuration gives rise to a high topography in the southwest corner and low topography in the northeast corner (Figure 9E), in this zone is located near Bocono city, according to Becke et al. [2005] with the lowest topography in the central part of the Venezuelan Andes. At the present time, the southern section of the Tuñame fault is normal, but for earlier ages (Pliocene) the fault was reversed. In figure 9F the gravimetric map shows high and low values in Tuñame and Burbusay wedge and conjugate expression in the north of the Valera and Burbusay faults, with a northwestern basin (this basin coincides with the location of La Sabana de Carora) and a high to the northeast, this basin and the topographic highs are originated due to the rotation of the block, caused by the movement of the Bocono fault to the south and the Oca Ancon fault to the north. Observing figure 4 there is a pattern of gravimetric highs and lows which has a trend from west to east even within Maracaibo Lake basin, as framed by the white line, it is possible that this configuration is diachronic and the age of the formation of the subbasins decreases from west to east, in the same way, this configuration is due to the movement of the Oca Ancon and Bocono faults. Therefore it is probable that traces of the Oca Ancon fault system are present further south than normally proposed. In the process of rotation and displacement of the Trujillo block along the Valera fault from the Pliocene, the granite of el Baño was exhumed, (Figure 9F) which has an AFT of 3 Ma [Baquero, 2015], therefore, the sub-basin located in La Sabana de Carora could have been formed at this time. Probably the last pulse in uplift of La Serrania de Trujillo could be associated with the interaction between northern of Maracaibo block and the area between the Valera and Burbusay faults, as a consequence of the thrust towards the northeast of the Boconó fault and the counterclockwise rotation of the Trujillo block. This configuration would cause reverse fault due to butressing effect in the east coast of Maracaibo Basin and Serrania de Trujillo. These reverse faults would have their origin in the upper crust lower crust boundary. In some cases, these deep efforts are manifested through preferential zones, such as the shale Colon formation, which constitute a detachment level in Merida Andes and Maracaibo Lake Basin.

An analog configuration is given by Christie-Blick and Biddle [1985] for San Andreas and San Jacinto faults in California. Evidence of a counterclockwise rotation in blocks to the northwest of a dextral slip strike fault is given by the work of Hernández et al. [2014]. It is considered a quasi-continuous block rotation model of the Patagonian Andes around the Liquiñe Ofqui fault zone based on paleomagnetic studies, also Backé et al. [2006] considers the sense of anticlockwise rotation of the Trujillo block which generates extension movements.

In figure 7, the fault system of the eastern cordillera of Colombia presents the same depths of Merida Andes from which it can be inferred that it has a common origin, that is, the mountain chain is the product of the inversion of Jurassic grabens such as the Uribante Graben to the south and the San Lazaro Graben to the north. There is controversy about the internal mechanism that causes the rise of the orogen, on the one hand there is Kellogg and Bonini [1982], DeToni and Kellogg [1993], Colletta et al. [1997] where they propose a thick skinned deformation model, that is, a mechanism where the upper basement is involved in conjunction with the sedimentary bodies, where it has a double vergence; while Yoris and Ostos [1997], Audemard and Audemard [2002], Cediel et al. [2003] and Monod [2010] have proposed a floating orogen model. Figure 7 shows sources with depths between 17 and 24 km associated with an uncoupling or detachment between the upper and lower crust that would cause the orogen formation. Therefore, it would be necessary to study the depth at which the event will occur, we can estimate the width of the Jurassic graben l_1 and a base h_1 (where h_1 would be associated with the base, this is the depth reached by the normal faults that produce the graben) the area $A1 = l_1 h_1$ after the rise of the orogen, $A2 = l_2 h_2$, according to Bermúdez et al. [2011] there is a rise of 1.7 km/m.y × 6 m.y more a second pulse of 0.4 km/m.y × 4 m.y produces a 11.8 km uplift; $h_2 = h_1 + 11.8$, if $A1 = A2$, [Dahlstrom 1969, Hossack, 1979; Mitra and Namson, 1987], $l_1 h_1 = l_2 h_2$ it can be deduced that

$$l_1 - l_2 = \left(\frac{h_1 + 11.8}{h_1} - 1\right) * l_2 \tag{2}$$

$l_1 - l_2$ represent shortening, l_2 the is the width of the profile 3 over the Andes approximately 90 km, the shortening according to Monod et al. [2011], Audemard and Audemard [2002] is approximately 45 km, Colleta et al. [1997], 50 to 60 km clearing h_1 we have.

$$h_1 = \frac{l_2 11.8}{l_1 - l_2} \approx 23 \text{ km} \tag{3}$$

This depth is associated with the upper and lower crust interface and therefore it would be in agreement with the proposed model of the floating orogen. Bermudez et al. [2010] indicate that the absence of deeply exhumed rocks appears more compatible with a shallow detachment underlying the mountain belt. However, Javadi et al. [2011] propose that the mylonitic rocks in the Andean were generated at 10 km or over 15 km depths.

A similar range of depths are found in the Eastern Cordillera of Colombia [Mora et al., 2008; Colleta et al., 1990; Cortés et al., 2006]. With the relationship described above and using the shortening data from Mora et al., 2008 for the profile located in figure 1 on the eastern mountain range of Colombia, with a total shortening ($l_1 - l_2$) of 58 km (Figure 4) calculated from line-length balancing in a cross section, ($l_2 \cdot h$) of 1330 km^2 results in a detachment a depth about 23 km in the undeformed state was obtained assuming the west-dipping fault as a main detachment [Mora et al., 2008], see figure 4 in that papers. This depth (23 km) for the detachment located between the upper crust and the lower crust found by Mora et al. [2008], Cortes et al. [2006] supports the relationship, between both mountain ranges and also the depths obtained in this paper.

It is interesting to note how both minimums are located at the ends of the "horse saddle" with which this geometric shape seems to be associated with the right lateral displacement of the Boconó fault. If the conservation of volume according to Dahlstrom [1969] is taken into account and clearing the depth of the base h_1 (associated with the Bocono fault) we obtain that

$$h_1 = \frac{E_2 l_2 11.8}{E_2(l_1 - l_2) - d_2[l_2 + (l_1 - l_2)]} = 23 \text{ km} \tag{4}$$

E_2 represents the length or extension of the Andes from the Colombia-Venezuela border to south of Barquisimeto is 470 km, d_2 is the displacement of the Boconó fault 60 km, therefore, the base would have to have a depth about 23 km, a fact that would rule out previous models where the fault of Boconó only reaches the upper crust and is in accordance with the range of depths reported on the map. This calculation evoked the concept of strain partitions. The instrumental seismicity, requires that the Bocono fault reaches the lowermost brittle crust at least and roots on an aseismic structure as a lower-crustal detachment at the rheological brittle-ductile transition in the crust to allow partitioning. In Audemard and Audemard [2002] the proposed models are restricted [Audemard, 1991; Kellogg and Bonini, 1982; De Toni and Kellogg, 1993; Castrillo, 1997, Colleta 1997, positive flower model of González de Juana 1952] to those where the Boconó fault reaches the base of the brittle crust or the brittle/ductile crust limit.

6. Conclusion

The basement map shows the asymmetry associated with the negative anomalies linked to the Maracaibo basin with 10 km of sedimentary thickness to the north and the Apure Barinas basin to the south with 5 km of thickness.

The 60 km of distance between the gravimetric minima of the basin of Lake Maracaibo and Apure Barinas is associated with the right lateral displacement of the Bocono fault.

Using spectral analysis, an interface was found, which is caused by a strong density contrast, this discontinuity or detachment located between the upper and lower crustal boundary would be associated with the seismogenic layer and all the fault systems that affect the Andean orogen probably have their origin in this discontinuity, this interface has a depth range of 17 to 24 km.

Base on the gravimetric response associated with this interface, 4 domains are defined; to the north related to the displacement of the Oca-Ancon fault and its influence on the Bonaire block, to the west the displacement of the Santa Marta Bucaramanga fault, to the east the Apure fault which is the limit between the Paleozoic and Precambrian basement and the central domain, linked with the Maracaibo block

The displacements of 60 km for the Bocono fault and 110 km for the Santa Marta Bucaramanga fault can be measured between the distance of structures located along the strike of these faults and associated with the upper crust lower crust interface.

After the Bocono fault system, the Oca Ancon system is the one with the greatest relevance since it is involved in the formation and reactivation of the main geological features that affect western Venezuela as a product of the interaction of the Caribbean plate to the north and the block of Maracaibo to the south. It is evident that there is a mechanical coupling between the Caribbean plate and the Maracaibo block.

The present-day distribution of the deformation in the Venezuelan Andes is consistent with strain partitioning and volume conservation. While compression is restricted on both flanks of the belt, strike-slip and extension occurs in the central part of the mountain range. The Andes of Merida is the product of the reactivation of the faults associated with the Jurassic grabens in conjunction with the low-angle faults which reach the limit between upper/lower crust, the San Lazaro and Uribante Grabens were separated as a result of the displacement of the Bocono fault which is in the range of 60 to 70 km, and compression about 50 to 60 km. The Uribante Graben continues to the southwest and joins the grabens that gave rise to the eastern cordillera of Colombia.

The first pulses of elevation in Oligocene time of the Andes of Mérida are due to the interaction of the Maracaibo block with the Caribbean plate and not with collision of the Panama arc.

It is possible that the uplift of the Merida Andes was dominated mainly by the northwest-southeast compression until 4 ma ago, then in the Pleistocene time the displacement of the Bocono fault and the rotation of the Trujillo block began to control the current structural configuration of the northeastern Andes

The Trujillo block evidences a counterclockwise rotation caused by the offset of the Bocono fault and movement of Oca Ancon fault, this configuration gives rise to a pattern of gravimetric lows and highs associated with subbasins and basement highs, located south of the Oca Ancon and north the Bocono fault and developed from east to west direction affecting the Maracaibo Lake basin. In this process of rotation and displacement of the Trujillo block along the Valera fault, the granite of el Baño was exhumed.

Data availability. The presented gravimetric data were recorded by the PDVSA Intevep. This original data remains confidential and the property of PDVSA.

Acknowledgements. xThe authors would like to thank the Project GIAME and its team for support during the research and Michael Schmitz for their thoughts on stages of the research and their motivation to finish the work.

References

Alberding, H. (1957). Application of principles of wrench-fault tectonics of Moody and Hill to northern South America, Bull. Geol. Soc. Am., 68, 785-790.

Araujo, F. (2013). Desarrollo e implementación de un código en matlab para realizar inversión de datos potenciales a través del análisis espectral. Tesis de maestría. Escuela de Geología, Minas y Geofísica. Departamento de Geología, Universidad Central de Venezuela, Caracas, 10,110.

Araujo, F. (2015). Interpretación gravimétrica de los andes de Mérida. Informe Interno para PDVSA Intevep, Caracas, 10-150.

Araujo, F. and N. Orihuela (2020). Integración y homologación de datos gravimétricos en el occidente de Venezuela para el cálculo de la anomalía de Bouguer de los Andes de Mérida, Rev. Técn. Ing., L.U.Z., 43, 2, 65-71, https://doi.org/10.22209/rt.v43n2a02.

Arnaíz, R.M. and F. Audemard (2014). Variations in elastic thickness and flexure of the Maracaibo block, J. S. Am. Earth Sci., 56, 251-264.

Arends, A., N. Díaz, G. Tang, D. Pinto, F. Mussa, A. Peraza, R. Rengifo, M. Pacheco, J. Fajardo, G. Tovar, M. Zambrano, A. Cragno, D. Escalona, D. Sánchez, N. Moreno and V. Padrón (2014). Geología y Potencial Hidrocarburífero del Golfo de Venezuela, Costa Afuera. Informe Confidencial para PDVSA, Caracas, 10-59.

Arnaiz, M. (2009). Modelado Gravimétrico Cortical de la Zona Noroccidental de Venezuela, Tesis de pregrado. Escuela de Geología, Minas y Geofísica. Departamento de Geología. Universidad Central de Venezuela, Caracas, 50-100.

Arnaiz, M., I. Rodríguez and F. Audemard (2011). Análisis gravimétrico y flexural del occidente de Venezuela, Revista Mexicana de Ciencias Geológicas, 28, 3, 420-438.

Audemard, F.A. (1998). Evolution géodynamique de la facade nord Sud-américaine: nouveaux apports de l'histoire geéologique du Bassin de Falcón, Vénézuéla. XIV Caribbean Geological Conference, Trinidad, 150-160.
Audemard, F.A. (1999). Morpho-structural expression of active thrust fault systems in humid tropical foothills of Colombia and Venezuela, Zeitschrift fuer Geomorphologie 118, 1-18.
Audemard, F.A. (2001). Quaternary tectonics and present stress tensor of the inverted northern Falcon Basin, northwestern Venezuela, J. Struct. Geol., 23, 2-3, 431-453.
Audemard, F.A. (1996). Paleoseismicity studies on the Oca-Ancon fault system, northwestern Venezuela, Tectonophysics, 259, 67-80.
Audemard, F.E. and F.A. Audemard (2002). Structure of the Mérida Andes, Venezuela relations with the South America-Caribbean geodynamic interaction, Tectonophysics, 345, 299-327.
Audemard, F.A. and C. Giraldo (1997). Desplazamientos dextrales a lo largo de la frontera meridional de la placa Caribe, Venezuela septentrional. Memorias del VIII Congreso Venezolano, Sociedad Venezolana de Geólogos, 1, 101-108.
Audemard, F.A., M. Machette, J. Cox, R. Dart and K. Halle (2000). Map and database of quaternary faults and folds in Venezuela and its offshore regions. Include map at scale 1:2.000.000, US Geological Survey, 78.
Audemard, F.A., G. Romero, H. Rendon and V. Cano (2005). Quaternary fault kinematics and stress tensors along the southern Caribbean from fault-slip data and focal mechanism solutions, Earth-Sci. Rev., 69, 181-233.
Audemard, F.E. (1991). Tectonics of Western Venezuela, PhD Thesis, Rice University, Houston, 245.
Backé, G., D. Dhont and Y. Hervouët (2006). Spatial and temporal relationships between compression, strike-slip and extension in the Central Venezuelan Andes: clues for Plio Quaternary tectonic escape, Tectonophysics, 425, 25-53.
Baquero, M. (2015). Evolución geodinámica del noroccidente de Venezuela, basado en nuevos datos de geocronología, geoquímica e isotópicos (Doctoral Dissertation). Universidad Central de Venezuela, Escuela de Geología, Geofísica y Minas, 1, 355.
Bermudez, M.A., B. Kohn, P. Van der Beek, M. Bernet, P. O'Sullivan and R. Shagam (2010). Spatial and temporal patterns of exhumation across the Venezuelan Andes: implications for Cenozoic Caribbean geodynamics, Tectonics, 29, 1-21.
Bermúdez, M.A., P. Van der Beek and M. Bernet (2011). Asynchronous Miocene-Pliocene exhumation of the central Venezuelan Andes, Geology, 39, 139-142.
Bermudez, M.A., P. Van Der Beek and M. Bernet (2013) Strong tectonic and weak climatic control on exhumation rates in the Venezuelan Andes, Lithosphere, 5, 3-16.
Bezada, M.J., M. Schmitz, M.I. Jácome, J. Rodríguez, F. Audemard, C. Izarra and the BOLIVAR Active Seismic Working Group (2008) Crustal structure in the Falcón Basin area, northwestern Venezuela, from seismic and gravimetric evidence, J. Geodyn., 45, 191-200.
Bird, P. (2003). An updated digital model of plate boundaries, Geochem. Geophys. Geosys, 4, doi:10.1029/2001GC000252.
Boinet, T., J. Bourgois, H. Mendoza and R. Vargas (1985). Le poinçon de Pamplona (Colombia), Un jalon de la frontière méridionale de la Plaque Carïbe. Bulletin de la Société Géologique de France, 1, 3, 403-413, https://doi.org/10.2113/gssgfbull.I.3.403.
Boinet, T., J. Bourgois, H. Mendoza and R. Vargas (1989). La Falla de Bucaramanga, Colombia, Su función durante la Orogenia Andina, Geología Norandina, 11, 3-10.
Bonini, W., C. Pimstein and V. Graterol (1977). Mapa de Anomalías Gravimétricas de Bouguer, Norte de Venezuela, mapa publicado por el Ministerio de Energía y Minas, Venezuela, Escala 1:1.000.000.
Campbell, C.J. (1968). The Santa Marta wrench fault and its regional setting: Transactions, 4th Caribbean Geological Conference, Port-of-Spain, Trinidad, 247-261.
Case, J.E., T. Holcombe and R.G. Martin (1984). Map of geologic provinces in the Caribbean region. In: Bonini, W. and R. Hargraves (eds.), The Caribbean-South American Plate Boundary and Regional Tectonics, GSA Memoir, Geological Society of America, Boulder, 162, 1-30.
Case, J.E., L. Duran, A. Lopez and W. Moore (1971). Tectonic investigations in western Colombia and eastern Panama, Bull. Geol. Soc. Am., 82, 2685-2712.
Case, J.E., R. Shagam and R.F. Giegengack (1990). Geology of the northern Andes: An overview, in The Geology of North America, vol. H, The Caribbean Region, edited by G. Dengo and J. E. Case, Geol. Soc. Am., Boulder, 177-200.
Castrillo, J. (1997). Structuration neogene du flanc nord-ouest des Andes venezueliennes entre Torondoy et Valera, PhD thesis, Universite de Pau et des Pays de l Adour, 247.

Cediel, F., R.P. Shaw and C. Cáceres (2003). Tectonic assembly of the Northern Andean Block, in The Circum Gulf of Mexico and the Caribbean: Hydrocarbon Habitats, Basin Formation, and Plate Tectonics, edited by C. Bartolini et al., AAAPG Mem, 79, 815-848.

Ceron, J., J. Kellogg and G. Ojeda (2007). Basement Configuration of the northwestern South America-Caribbean margin from recent geophysical data, Cienc. Tecnol. Futuro 3, 3, 25-49

Chiarabba, C., P. De Gori, C. Faccenna, F. Speranza, D. Seccia, V. Dionicio and G.A. Prieto (2015). Subduction system and flat slab beneath the Eastern Cordillera of Colombia, Geochem. Geophys. Geosys, 17, 16-27.

Christie-Blick, N. and K.T. Biddle (1985). Deformation and basin formation along strike-slip faults. In: Biddle, K.T. and N. Christie-Blick (eds.), Strike-Slip Deformation, Basin Formation, and Sedimentation, SEPM Special Publication, 37, 1-34.

Cisneros, M. (2016). Modelado gravimétrico 2D del perfil central del proyecto Giame en el noroccidente Venezolano. Tesis de pregrado presentada ante la Universidad Simón Bolívar, Departamento de Geofísica, 10-50.

Colleta, B., F. Hebrard, J. Letouzey, P. Werner and J.L. Rudkiweicz (1990). Tectonic style and crustal structure of the Eastern Cordillera, Colombia from a balanced cross section. In: Letouzey, J. (ed.), Petroleum and tectonics in mobile belts: Paris, Editions Technip, 81-100.

Colletta, B., F. Roure, B. De Toni, D. Loureiro, H. Passalacqua and Y. Gou (1997). Tectonic inheritance, crustal architecture, and contrasting structural styles in the Venezuelan Andes, Tectonics, 16, 5, 777-794.

Cordell, L. and R.G. Henderson (1973). Gravity analysis using an exponential density depth function-San Jacinto Graben, California, Geophys., 38, 4, 684-690.

Corredor, F. (2003). Eastward extent of the Late Eocene- Early Oligocene onset of deformation across the northern Andes: Constraints from the northern portion of the Eastern Cordillera fold belt, Colombia, J. South Am. Earth Sci., 16, 445-457, doi:10.1016/j.jsames.2003.06.002.

Cortés, M., G. Bayona, J. Aristizabal, G. Ojeda, A. Reyes-Harker and N. Gamba (2006). Structure and kinematics of the Eastern Foothills of the Eastern Cordillera of Colombia from balanced cross-sections and forward modeling: Extended Abstracts, IX Simposio Bolivariano de Exploración Petrolera en las Cuencas Subandinas, Cartagena de Indias, Colombia, 10-20.

Cruces-Zabala J., O. Ritter, U. Weckmann, K. Tietze, N. Meqbel, F. Audemard and M. Schmitz (2022). Three-dimensional magnetotelluric imaging of the Mérida Andes, Venezuela J. South Am. Earth Sci., 11,4, 10-37.

De Ratmiroff, G. (1970). Late Cenozoic imbricate thrusting in Venezuelan Andes, Bull. Am. Assoc. Pet. Geol., 55, 1336-1344.

De Toni, B. and J. Kellogg (1993). Seismic evidence for blind thrusting of the northwestern flank of the Venezuelan Andes, Tectonics, 12, 6, 1393-1409.

Dewey, J. (1972). Seismicity and tectonics of western Venezuela, Bull. Seismol. Soc. Am., 62, 6, 1711-1751.

Dahlstrom, C.D.A. (1969). Balanced cross sections: Canadian Journal of Earth Sciences, v. 6, Structural geology in the eastern margin of the Canadian Rocky Mountains, Bull. Canadian Petroleum Geologists, 18, 332-406.

Dhont, D., G. Backé and Y. Hervouët (2005a). Plio-Quaternary extension in the Venezuelan Andes: mapping from SAR JERS imagery, Tectonophysics, 399, 293-312.

Dimitriadis, K., G.A. Tselentis and K. Thanassoulas (1987). A basic program for 2-D spectral analysis of gravity data and source-depth estimation, Compu. Geosci., 13, 5, 549-560.

Diederix, H., O.P. Bohórquez, H. Mora-Páez, J.R. Peláez, L. Cardona, Y. Corchuelo, J. Ramírez and F. Díaz-Mila (2020). Quaternary activity of the Bucaramanga Fault in the Departments of Santander and Cesar. In: Gómez, J. and A.O. Pinilla-Pachon (editors), The Geology of Colombia, Volume 4 Quaternary. Servicio Geológico Colombiano, Publicaciones Geológicas Especiales 38, 453-477, https://doi.org/10.32685/pub.esp.38.2019.13.

Duerto, L., A. Escalona and P. Mann (2006). Deep structure of the Mérida Andes and Sierra de Perijá mountain fronts, Maracaibo Basin, Venezuela, AAPG Bulletin, 90, 505-528, doi: 10.1306/10080505033.

Ellis, S. (1996). Forces driving continental collision: reconciling indentation and mantle subduction tectonics, Geology, 24, 699-702.

Escalona, A. and P. Mann (2003). Three-dimensional structural architecture and evolution of the Eocene pull-apart basin, central Maracaibo basin, Venezuela, Marine and Petroleum Geology, 20, 2, 141-161.

Escalona, A. and P. Mann (2006). An overview of the petroleum system of Maracaibo Basin, AAPG Bulletin, 90, 657-678.

Escalona, A. and P. Mann (2011). Tectonics, basin subsidence mechanics, and paleogeography of the Caribbean-South American plate boundary zone, J. Marine Petrol. Geol., 28, 8-39, https://doi.org/10.1016/j.marpetgeo.2010.01.016

Escobar, A. and I. Rodríguez (1995). Interpretación geofísica integrada de un transecto NW-SE a través de los andes venezolanos, I Latinoamerican Geophysical Congress, Rio de Janeiro, Brazil, 273-276.

Etayo, F. and C. Rodrıguez (1985). Edad de la Formacion Los Santos, Proyecto Cretacico INGEOMINAS, Publicacion Especial, 16, 1-13.

Estévez, R. and J. Laffaille (2010). Sismicidad y prevención sísmica en los Andes Venezolanos. http://www.funvisis.gob.ve/old/archivos/www/terremoto/Papers/Doc029/doc029.htm

Feo-Codecido, G. (1972). Breves ideas sobre la estructura de la Falla de Oca, Venezuela: VI Conferencia Geológica del Caribe, Margarita, Memoria, 184-190.

Feo-Codecido, G., F. Smith, N. Aboud and E. Di Giacomo (1984). Basement and Paleozoic rocks of the Venezuelan Llanos Basin, Geol. Soc. Am. Memoir, 162, 175-187.

Folinsbee, R.A. (1972). The gravity field and plate boundaries in Venezuela (Ph.D. dissertation). Mass. Inst. of Technology – Wodds Hole Oceanog. Inst, 160.

Freymueller, J.T., J.N. Kellogg and V. Vega (1993). Plate motions in the north Andean region, J. Geophys. Res., 98, 21, 853-21, 863.

García, A. (2009). Mapas de anomalías de gravedad y magnetismo de Venezuela generados a partir de datos satelitales. Trabajo de Grado, Universidad Central de Venezuela, 208.

Giegengack, R. (1984). Late Cenozoic tectonic environments of the central Venezuelan Andes, Mem. Geol. Soc. Am., 162, 343-364.

Giraldo, C. (1996) Hipotesis acerca del desplazamiento de la Falla del Pilar, Venezuela Nororiental: VIII Congreso Venezolano de Geofısica, Tectonica, Maracaibo, Venezuela, 387-392.

Gorney, D., A. Escalona, P. Mann, M.B. Magnani and Bolivar Study Group (2007). Chronology of Cenozoic tectonic events in western Venezuela and the Leeward Antilles based on integration of offshore seismic reflection data and on-land geology, AAPG Bulletin, 91, 5, 653-684.

González de Juana, C. (1952). Introducción al estudio de la geología de Venezuela, Boletín de Geología, Caracas, 2, 407-416.

González de Juana, C., J. Iturralde and X. Picard (1980). Geología de Venezuela y de sus Cuencas Petrolíferas, Caracas, Ediciones Foninves, 1100.

Gótze, H., M. Schmitz, P. Giese, S. Schmidt, P. Wigger, G. Schwarz, M. Araneda, G. Chong and J. Víramonte (1995). Las estructuras litosférícas de los Andes Centrales australes basadas en interpretaciones geofísicas, una revisión, Revista Geológica de Chile, 22, 2, 179-192.

Grande, S. (2013). Terreno Falconia: bloque alóctono Neoproterozoico de alto grado metamórfico, en el Noroccidente de Venezuela, Rev. Venezolana de Ciencias de la Tierra, 45, 1-22.

Grande, S. and F. Urbani (2009). Presence of high-grade rocks in NW Venezuela of possible Grenvillian affinity. In: James, K.H., M.A. Lorente and J.L. Pindell (eds.), The origin and evolution of the Caribbean plate, Geological Society, London, Special Publications, 328, 533-548.

Graterol, V. and W. Gumert (1998). 3-D gravity inversion with variable datum, The Leading Edge, 17, 12, 1769-1772.

Guzman, J.I. and W.L. Fisher (2006) Early and middle Miocene depositional history of the Maracaibo basin, western Venezuela, Am. Assoc. Pet. Geol. Bull., 90, 625-655.

Hackley, P.C., F. Urbani, A. Karlsen and C. Garrity (2006). Geological shaded relief map of Venezuela, Tech. rept. U.S. Geological Survey.

Hervouët, Y., J.T. Castrillo-Delgado and O. Odreman (2001). Interaction entre un chevauchement imbrique et une zone transcurrente; le flanc nord-ouest de Andes venezueliennes, Bulletin de la Societe Geologique de France, 172, 2, 159-175.

Hoorn, C., J. Guerrero, G.A. Sarmiento and M.A. Lorente (1995). Andean tectonics as a cause for changing drainage patterns in Miocene northern South America, Geology, 23, 237-240, doi: 10.1130/0091-7613(1995)023<0237:ATAACF>2.3.CO;2

Hossack, J.R. (1979). The use of balanced crosssections in the calculation of orogenic contraction: a review, J. Geol. Soc. London, 136, 705-711.

Hospers, J. and J.C. Van Wijnen (1958). Rock Densities of The Central Venezuelan Andes. Geological Society of America Bulletin, 69, 3, 359-362, doi: 10.1130/0016-7606(1958)69[359:rdotcv]2.0.co;2.

Ibañez-Mejía M., J. Ruiz, V. Valencia, A. Cardona, G.E. Gehrels and A. Mora (2011).The Putumayo Orogen of Amazónico and its implications for Rodinia reconstructions: New U-Pb geochronological insights into the Proterozoic tectonic evolution of northwestern South America, Precambrian Research, 191, 1-2, 58-77.

James, K.H. (1990). The Venezuelan Hydrocarbon Habitat. In: Brooks, J. (ed.), Classic Petroleum Provinces, Geol. Soc. Lond. Spec. Publ, 50, 9-35.

James, K.H. (2000). The Venezuelan hydrocarbon habitat. Part 1: Tectonics, structure, palaeogeography and source rocks, J. Petrol. Geol., 23, 5-53.

Javadi, H.R., M. Foroutan, M.E. Ashtiani, J.A. Urbina, A. Saidi and M. Faridi (2011). Tectonics changes in NW South American Plate and their effect on the movement pattern of the Boconó Fault System during the Mérida Andes evolution, J. South Am. Earth Sci., 32, 14-29, https://doi.org/10.1016/j.jsames.2011.04.008

Kellogg, J. (1984). Cenozoic tectonic history of the Sierra de Perijá, Venezuela-Colombia, and adjacent basins. In: Bonini, W., R. Hargraves and R. Shagam (eds.), The Caribbean-South American plate boundary and regional tectonics. Boulder, CO: Mem. Geol. Soc. Am., 162, 239-261.

Kellogg, J.N. and W.E. Bonini (1982). Subduction of the Caribbean plate and basement uplifts in the overriding South American plate, Tectonics, 1, 3, 251-276.

Kohn, B., R. Shagam, P. Banks and L. Burkley (1984). Mesozoic-Pleistocene fission track ages on rocks of the Venezuelan Andes and their tectonic implications, Mem. Geol. Soc. Am., 162, 365-384.

La Fehr, T.R. (1991). Standardization in gravity reduction, Geophys., 56, 1170, doi: 10.1190/1.1443137

Laubscher, H.P. (1987). The kinematic puzzle of the Neogene northern Andes. In: Schaer, J.P. and J. Rodgers (editors), The anatomy of mountain ranges. Princeton University Press, Princeton, USA, 211-228, https://doi.org/10.1515/9781400858644.211

Linares, F., D. Arnaiz, N. Orihuela (2015). Mapa de anomalías de Bouguer de Venezuela derivado del modelo combinado EIGEN-6C4, Geociencias Aplicadas Latinoamericanas, 25, 205-215.

Lugo, J. and P. Mann (1995). Jurassic-Eocene Tectonic Evolution of Maracaibo Basin, AAPG Memoir, 62, 699-725.

Macellari, C. (1984). Late Tertiary tectonic history of the Táchira Depression, southwestern Venezuelan Andes, Mem. Geol. Soc. Am., 162, 333-340.

Macellari, C.E. (1995). Cenozoic sedimentation and tectonics of the Southwestern Caribbean pull-apart basins, Venezuela and Colombia. In: Tankard A., R.S. Suarez and H.J. Welsink (eds.), Petroleum basins of South America, AAPG Memoir, 62, 757-780.

Mcmahon, C.E. (2000). Evaluation of the effects of oblique collision between the Caribbean and South American plates using geochemistry from igneous and metamorphic bodies of Northern Venezuela. Phd Dissertation. University Notre Dame, Indiana, USA, 227.

Mann, P. and K. Burke (1984). Neotectonics of the Caribbean, Rev. Geophys., 22, 4, 309-362.

Mann, P., C. Schubert and K. Burke (1990). The Caribbean Region. Dengo,J. E. (ed), Review of Caribbean neotectonics. Boulder, CO, Geol. Soc. Am., 307-338.

Mann, P., A. Escalona and M.V. Castillo (2006). Regional geologic and tectonic setting of the Maracaibo supergiant basin, western Venezuela, AAPG Bulletin, 99, 4, 445-477.

Maresch, W.V., B. Stoeckhert, A. Baumann, C. Kaiser, R. Kluge, G. Krueckhans-Lueder, M.R. Brix and M. Thomson (2000). Crustal history and plate tectonic development in the southern Caribbean, Zeitschrift fuer Angewandte Geologie, 1, 283-289.

Mattauer, M. (1983). Subduction de lithosphere continentale, decollement croute-manteau et chevauchement dechelle crustale dans la chaıne de collision himalayenne, Comp. Ren. de Acad. Sci., Paris, 296, 481-486.

Mattauer, M. (1985). Intracontinental subduction, crust-mantle decollement and crustal stacking wedge in the Himalaya and other collision belts. Collision Tectonics, Geol. Soc. Sp. Pub., Geol. Soc. London, 14, 363-385.

Mazuera, F., M. Schmitz, A. Escalona, C. Zelt and A. Levander (2019). Lithospheric structure of northwestern Venezuela from wide-angle seismic data: Implications for the understanding of continental margin evolution, Journal of Geophysical Research, Solid Earth, 124, https://doi.org/10.1029/2019JB017892.

Mishra, D.C. and P.S. Naidu (1974). Two-dimensional power spectral analysis of aeromagnetic fields, Geophys. Prosp., 22, 345-353.

Mitra, S. and J. Namson (1987). Limitations and modifications of area balancing methods: I Excess area method, Geological Society of America abstracts with programs, 19, 774.

Monod, B., D. Dhont and Y. Hervouët (2011). Orogenic float of the Venezuelan Andes, Tectonophysics, 490, 123-135.

Mora, A., M. Parra, M.R. Strecker, E.R. Sobel, H. Hooghiemstra, V. Torres, H. Vallejo and J. Jaramillo (2008). Climatic forcing of asymmetric orogenic evolution in the Eastern Cordillera of Colombia. GSA Bulletin 120, 7/8, 930-949.

Mora-Paez, H., L. Giraldo-Londono, L. Cardona-Piedrahita, J. Pelaez-Gaviria and S. Lizarazo (2016a). Velocidades geodesicas horizontales de Colombia, Grupo de Investigaciones Geodesicas Espaciales, Proyecto GeoRED, Servicio Geologico Colombiano, Documento Interno, Bogota.

Mora, A., M. Ibañez-Mejia, O. Oncken, M. De Freitas, V. Vélez, A. Mesa and L. Serna (2017). Structure and age of the Lower Magdalena Valley Basin basement, northern Colombia: New reflection-seismic and U-Pb-Hf insights into the termination of the central Andes against the Caribbean Basin, J. South Am. Earth Sci., 74, 1-26, https://doi.org/10.1016/j.jsames.2017.01.001

Montes, C., R.D. Hatcher and P. Restrepo-Pace (2005). Tectonic reconstruction of the northern Andean blocks: Oblique convergence and rotations derived from the kinematics of the Piedras Girardot area, Colombia, Tectonophysics, 399, 221-250, doi:10.1016/j.tecto.2004.12.024.

Muessig, K. (1984). Structure and Cenozoic tectonics of the Falcon Basin, Venezuela, and adjacent areas. In: Tankard, A., S. Suarez, and H. Welsink (eds.), Petroleum basins of South America, AAPG Memoir 62, 217-230.

Narasimha-Rao, B., P. Rama-Krishna and A. Markandeyulu (1996). Mapros-A computer program for basement mapping and filtering of gravity and magnetic data using a hartley transform, Compu. Geosci., 22, 3, 117-218.

Orihuela, N. (2014). Historia de la gravimetría en Venezuela, Revista Venezolana de Ciencias de la Tierra, 46, 1, 44-57.

Orihuela-Guevara, N., A. García and T. Tabare (2011). Mapas de gravedad y anomalía gravimétrica de Venezuela derivados de datos satelitales, Revista de la Facultad de Ingeniería, Universidad Central de Venezuela, 26, 1, 77-85.

Palme, C., M. Morandi and J. Choy (2005). Reevaluación de las intensidades de los grandes sismos históricos de la región de la cordillera de Mérida utilizando el método de Bakun y Wentworth, Revista Geográfica Venezolana, número especial.

Pérez, O.J and J.S. Mendoza (1998). Sismicidad y tectónica en Venezuela y áreas vecinas. Revista. Física de la Tierra, 10, 87.

Pérez, O.J., M. Jaimes, E. Garciacaro (1997). Microseismicity evidence for subduction of the Caribbean plate beneath the South American plate in northwestern Venezuela, J. Geophys. Res.,102, B8,17875-17882.

Pérez, O.J., R. Bilham, R. Bendick, J. Velandia, C. Hernandez, M. Hoyer and M. Kozuch (2001). Velocity field across the southern Caribbean plate boundary and estimates of Caribbean-South American plate motion using GPS geodesy 1994-2000, Geophys. Res. Lett., 28, 2987-2990.

Pérez, O.J., R. Bilham, M. Sequera, L. Molina, P. Gavotti, H. Codallo, C. Moncayo, C. Rodríguez, R. Velandia, M. Guzmán and P. Molnar (2011). Campo de Velocidades GPS en el Occidente de Venezuela: Componente lateral derecha asociada a la Falla de Boconó y componente convergente perpendicular a Los Andes, Interciencia, 36,1, 39-44.

Pérez, O.J., S.G. Wesnousky, R. De La Rosa, J. Márquez, R. Uzcátegui and C. Quintero (2018). On the interaction of the North Andes plate with the Caribbean and South American plates in northwestern South America from GPS geodesy and seismic data, Geophys. J. Int., 214, 1986-2001, https://doi.org/10.1093/gji/ggy230.

Pindell, J. and L. Kennan (2001). Kinematic evolution of the Gulf of Mexico and Caribbean, in Petroleum Systems of Deep-Water Basins: Global and Gulf of Mexico Experience: GCSSEPM Foundation, 21st Annual Research Conference, Houston, Texas,GSSEPM, 193-220.

Pindell, J.L., L. Kennan, W.V. Maresch, K.P. Stanek, G. Draper and R. Higgs (2005). Plate kinematics and crustal dynamics of circum-Caribbean arc-continent interactions, and tectonic controls on basin development in proto-Caribbean margins. In: Ave-Lallemant, H.G. and V.B. Sisson (eds.), Caribbean-South American Plate Interactions, Venezuela. Geol. Soc. Am. Spec. Papers, 394, 7-52.

Pindell, J.L. and L. Kennan (2009). Tectonic evolution of the Gulf of Mexico, Caribbean and northern South America in the mantle reference frame: An update. In: James, K.H., M.A. Lorente and J.L. Pindell (eds.), The Origin and evolution of the Caribbean Plate, Geol. Soc. [London] Spec. Pub., 328, 1-55.

Parnaud, F., Y. Gou, J.C. Pascual, M.A. Capello, Y. Truskowski, H. Passalacqua and F. Roure (1995). Stratigraphic Synthesis of Western Venezuela. In: Tankard, A., R. Suárez and H.J. Welsink, Petroleum Basins of South America, AAPG Mem, 62, 681-698.

Priem, H.N.A., D.J. Beets and E.A.T. Verdurmen (1986). Precambrian rocks in an early Tertiary conglomerate on Bonaire, Netherlands Antilles (southern Caribbean borderland); evidence for a 300 km eastward displacement relative to the South American mainland?. Geologie en Mijnbouw, Amsterdam, 65, 1, 35-40.

Reid, A.B., J.M. Allsop, H. Granser, A.J. Millett and I.W. Somerton (1990). Magnetic interpretation in three dimensions using Euler deconvolution, Geophys., 55, 80-91.

Rod, E. (1956). Strike Slip Faults of Northern Venezuela, AAPG Bulletin, 40, 3, 457-465.

Sánchez-Rojas, J. (2011). New Bouguer gravity maps of Venezuela: representation and analysis of free air and Bouguer anomalies with emphasis on spectral analyses and elastic thickness, Int. J. Geophys., 2012, 1-19.

Sánchez-Rojas, J. and M. Palma (2014). Crustal density structure in northwestern South America derived from analysis and 3-D modelling of gravity and seismicity data, Tectonophysics, 634, 97-115, https://doi.org/10.1016/j.tecto.2014.07.026.

Sandwell, D.T. and W.H.F. Smith (1997). Marine gravity anomaly from Geosat and ERS-1 satellite altimetry, J. Geophys. Res., 102, 10, 039-10, 054, doi:10.1029/96JB03223

Sandwell, D.T., R.D. Müller, W.H.F. Smith, E. Garcia and R. Francis (2014). New global marine gravity model from CryoSat-2 and Jason-1 reveals buried tectonic structure, Science, 346, 65-67, doi: 10.1126/science.1258213.

Schmitz, M., N. Orihuela, J. Choy, E. Gil, F. Mazuera, J. Sánchez, F. Audemard, M. Arnaíz, C. Reinoza, F. Araujo, O. Ritter, A. Levander, F. Niu, J. Avila, K. García, L. Yegres, J. Cruces, M. Cerrada, J. González, G. Barreto, H. Rendon, M. Bolívar, Y. Molero and J. Lara (2015). Investigaciones geofísicas integradas para estudiar la estructura litosférica de Los Andes de Mérida. X Congreso de CONVESIS, Cumana, 12.

Schubert, C. (1982). Neotectonics of the Bocono fault, western Venezuela, Tectonophysics 85, 205-220.

Schubert, C.Y. and L. Vivas (1993). El Cuaternario de la Cordillera de Mérida. Andes Venezolanos, Universidad de Los Andes. Fundación Polar. Mérida Venezuela, 345.

Shagam, R., B.P. Kohn, P. Banks, L. Dasch, R. Vargas, G. Rodríguez and N. Pimentel (1984). Tectonic implications of Cretaceous-Pliocene fission track ages from rocks of the circum-Maracaibo Basin region of western Venezuela and eastern Colombia, Mem. Geol. Soc. Am., 162, 385-412.

Silver, E.A., J.E. Case and H.J. MacGillavry (1975). Geophysical study of the Venezuelan borderland, Geol. Soc. Am. Bull., 86, 2, 213-226.

Smith, F. (1980). El Basamento y las Rocas Paleozoicas en la parte norte de Venezuela. Gerencia de estudios especiales e investigación, Informe Técnico para Corpoven, 60.

Spector, A. and F.S. Grant (1970). Statistical methods for interpreting aeromagnetic data. Geophys., 35, 293-302.

Stephan, J.F. (1985). Andes et chaine caraïbe sur la transversal de Barquisimento (Venezuela), Proceedings of Symposium Géodynamique des Caraïbes, 505-529.

Stephan, J.F. (1982). Evolution géodynamique du domaine Caraïbe, Andes et chaine Caraïbe sur la transversale de Barquisimeto (Venezuela), Univ. Pierre et Marie Curie (Paris VI). These doctorat d´etat.

Soulas, J.-P. and A. Singer (1987). Evidencias de actividad cuaternaria en las fallas. In: Soulas, J.-P., A. Singer and M. Lugo (1987), Tectonica cuaternaria, caracterısticas sismogenicas de las fallas de Bocono, San Simon y del piedemonte occidental andino y efectos geologicos asociados a la sismicidad historica (Proyecto Sumandes), Funvisis unpublished report for Maraven S.A, 90.

Taboada, A., L.A. Rivera, A.S. Fuenzalida, A. Cisternas, H. Philip, H. Bijwaard, J. Olaya and C. Rivera (2000). Geodynamics of the northern Andes: Subductions and intracontinental deformation (Colombia), Tectonics, 19, 787-813.

Toro, J. (1990). The termination of the Bucaramanga Fault in the Cordillera Oriental, Colombia: Masters Thesis, University of Arizona, Department of Geosciences, Tucson, 60.

Thompson, D.T. (1982). EULDPH: a new technique for making computer-assisted depth estimates from magnetic data, Geophys., 47, 31-37.

Toto, E.A. and J.N. Kellogg (1992). Structure of the Sinu-San Jacinto fold belt-An active accretionary prism in northern Colombia, J. South Am. Earth Sci., 5, 1, 211-222.

Trenkamp, R., J.N. Kellogg, J.T. Freymueller and H. Mora (2002). Wide plate margin deformation, southern Central America and northwestern South America, CASA GPS observations, J. South Am. Earth Sci., 15, 157-171.

Tschanz, C.M., R.F. Marvin, J. Cruz, H. Mehnert and G. Cebulla (1974). Geologic Evolution of the Sierra Nevada de Santa Marta area, Colombia: Geological Society of America Bulletin, 85, 273-284.

Ujueta, G. (2003). La Falla de Santa Marta-Bucaramanga no es una sola falla; son dos fallas diferentes: La Falla de Santa Marta y la Falla de Bucaramanga, Geología Colombiana, 28, 133-153.

Urbani, F., S. Grande and J. Méndez-Baamonde (2013). Petrography of exotic clasts in the soebi blanco formation, bonaire, netherlands Antilles, Boletín de Ciencias de la Tierra, 59-70.

Van der Lelij, R., R. Spikings, A. Kerr, C. Andrew, A. Kounov, M. Cosca, D. Chew and D. Villagomez (2010). Thermochronology and tectonics of the Leeward Antilles: Evolution of the southern Caribbean Plate boundary zone, Tectonics, 29, 6, doi: 10.1029/2009TC002654

Vasquez, E.E. and P.A. Dickey (1972). Major faulting in north-western Venezuela and its relation to global tectonics: VI Caribbean Geological Conference, Margarita,Venezuela, Transactions, 191-202.
Von der Osten, E. and D. Zozaya (1957). Geologfa de la parte suroeste de1 Estado Lara, region de Qufbor (Carta 2308), Bol. Geol. (Venezuela), 4, 3-52.
Wright, J. and S. Wild (2011). Late Cretaceous subduction initiation on the eastern of the Caribbean-Colombian Oceanic Plateau: One Great Arc of the Caribbean?, Geosphere, 7, 2, 1-26.
Yoris, F. and M. Ostos (1997). Geology of Venezuela: General Geology and Oil Basins, of: Singer, J. (ed), WEC 1997 Well Evaluation Conference. Schlumberger-Surenco, CA, 1-17.

***CORRESPONDING AUTHOR: Francisco ARAUJO**,
Universidad Central de Venezuela, Facultad de Ingeniería, Departamento de Ingeniería Geofísica,
PDVSA Intevep, Gerencia de Exploración y Caracterización de Yacimientos
e-mail: franck074@gmail.com, araujofp@pdvsa.com